



Development of Brain Injury Criteria (BrIC)

Erik G. Takhounts, Matthew J. Craig, Kevin Moorhouse, Joe McFadden
National Highway Traffic Safety Administration

Vikas Hasija
Bowhead Systems Management, Inc.

ABSTRACT – Rotational motion of the head as a mechanism for brain injury was proposed back in the 1940s. Since then a multitude of research studies by various institutions were conducted to confirm/reject this hypothesis. Most of the studies were conducted on animals and concluded that rotational kinematics experienced by the animal’s head may cause axonal deformations large enough to induce their functional deficit. Other studies utilized physical and mathematical models of human and animal heads to derive brain injury criteria based on deformation/pressure histories computed from their models. This study differs from the previous research in the following ways: first, it uses two different detailed mathematical models of human head (SIMon and GHBMC), each validated against various human brain response datasets; then establishes physical (strain and stress based) injury criteria for various types of brain injury based on scaled animal injury data; and finally, uses Anthropomorphic Test Devices (ATDs) (Hybrid III 50th Male, Hybrid III 5th Female, THOR 50th Male, ES-2re, SID-IIs, WorldSID 50th Male, and WorldSID 5th Female) test data (NCAP, pendulum, and frontal offset tests) to establish a kinematically based brain injury criterion (BrIC) for all ATDs. Similar procedures were applied to college football data where thousands of head impacts were recorded using a six degrees of freedom (6 DOF) instrumented helmet system. Since animal injury data used in derivation of BrIC were predominantly for diffuse axonal injury (DAI) type, which is currently an AIS 4+ injury, cumulative strain damage measure (CSDM) and maximum principal strain (MPS) were used to derive risk curves for AIS 4+ anatomic brain injuries. The AIS 1+, 2+, 3+, and 5+ risk curves for CSDM and MPS were then computed using the ratios between corresponding risk curves for head injury criterion (HIC) at a 50% risk. The risk curves for BrIC were then obtained from CSDM and MPS risk curves using the linear relationship between CSDM - BrIC and MPS - BrIC respectively. AIS 3+, 4+ and 5+ field risk of anatomic brain injuries was also estimated using the National Automotive Sampling System - Crashworthiness Data System (NASS-CDS) database for crash conditions similar to the frontal NCAP and side impact conditions that the ATDs were tested in. This was done to assess the risk curve ratios derived from HIC risk curves. The results of the study indicated that: (1) the two available human head models – SIMon and GHBMC – were found to be highly correlated when CSDMs and max principal strains were compared; (2) BrIC correlates best to both - CSDM and MPS, and rotational velocity (not rotational acceleration) is the mechanism for brain injuries; and (3) the critical values for angular velocity are directionally dependent, and are independent of the ATD used for measuring them. The newly developed brain injury criterion is a complement to the existing HIC, which is based on translational accelerations. Together, the two criteria may be able to capture most brain injuries and skull fractures occurring in automotive or any other impact environment. One of the main limitations for any brain injury criterion, including BrIC, is the lack of human injury data to validate the criteria against, although some approximation for AIS 2+ injury is given based on the angular velocities calculated at 50% probability of concussion in college football players instrumented with 5 DOF helmet system. Despite the limitations, a new kinematic rotational brain injury criterion – BrIC – may offer a way to capture brain injuries in situations when using translational accelerations based HIC alone may not be sufficient.

KEYWORDS – brain injury criteria, finite element modeling of brain, SIMon, GHBMC, risk curves

INTRODUCTION

According to the Centers for Disease Control and Prevention (CDC) traumatic brain injury (TBI) is an

important public health problem in the United States. TBI is frequently referred to as the “silent epidemic” because the complications from TBI, such as changes affecting thinking, sensation, language, or emotions,

Address correspondence to Erik G Takhounts, Ph.D., USDOT, 1200 New Jersey Avenue, SE Washington, D.C. 20590. Electronic mail: erik.takhounts@dot.gov

may not be readily apparent. The most recent CDC report (Frieden et. al, 2010) estimates 1.7 million people sustain a TBI annually, of them 52,000 die.

The report finds that among all age groups, motor vehicle-traffic (MVT) was the second leading cause of TBI (17.3%) and resulted in the largest percentage of TBI-related deaths (31.8%).

Based on National Automotive Sampling System – Crashworthiness Data System (NASS-CDS) analyses of tow-away crashes (Eigen and Martin, 2005), fatalities attributable to head injuries are second only to fatalities attributable to thoracic region with societal costs exceeding \$60 billion.

Utilizing NASS-CDS from 1997 to 2011, a weighted annual estimate for AIS 3+ anatomic brain injuries averaged roughly 6500 cases with that value remaining as high as 9000 cases per year as recently as 2010. This was a population limited to belted occupants 15 and older in crashes where the most severe event was a frontal and side impact without rollover. Figure 1 shows the annual average risk of AIS 3+, 4+, and 5+ anatomic brain injuries from 1999 to 2011. Note, the percent risk is a running three year average (e.g., 1999 is the average risk from 1997 to 1999 and so on) and, per above, includes all frontal, near-side, and far-side crashes involving age 15 and older, belted occupants. Model years were restricted to “newer” vehicles in each case year by limiting model years to the case year minus 10. It can be seen from Figure 1 that the weighted risk of AIS 3+, 4+, and 5+ anatomic brain injuries, if anything, has been increasing over the last decade.

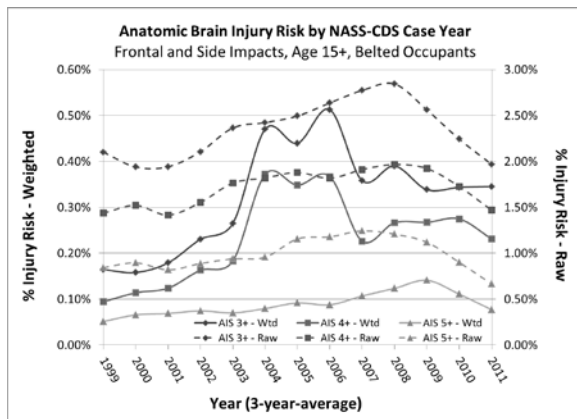


Figure 1. Anatomic brain injury risk in frontal and side impact tow-away crashes in NASS-CDS.

Many attempts have been made in the past to reduce the occurrence and severity of TBI in automotive crashes. Among them are design and development of improved safety systems governed by various Federal Motor Vehicle Safety Standards (FMVSS), requirements of the New Car Assessment Program (NCAP), tests of Insurance Institute for Highway

Safety (IIHS), and others. However, despite of all these requirements TBI is still one of the most frequent injury types in motor vehicle crashes (Eigen and Martin, 2005). The reasons for this may be multiple: (1) the mandatory and voluntary requirements may not capture some real world crash scenarios leading to TBI, (2) the Anthropomorphic Test Devices (ATDs) used in these tests are not interacting with vehicle environment in the way humans do, and (3) the interpretation of the ATDs' measurements is not sufficient to capture all possible types of TBI.

It is reason 3 that is investigated in this paper with the focus on the rotationally induced anatomic brain injuries. First, we make use of the scaled animal data (Abel et al., 1978; Stalnaker et al., 1977; Meaney et al., 1993) along with the National Highway Traffic Safety Administration (NHTSA) developed finite element (FE) model of human brain, i.e. the simulated injury monitor (SIMon) and its biomechanical injury criteria for diffuse axonal injury (DAI) type brain injuries – cumulative strain damage measure (CSDM) (Takhounts et al., 2003 and 2008) and maximum principal strain (MPS); as well as the head model developed by the Global Human Body Modeling Consortium, LLC (GHBMC) with the same injury criteria (Mao et al., 2013). Then, assuming DAI type anatomic brain injuries in animals (over 15 minutes loss of consciousness, severe hematoma, etc., along with the AIS 4+ injuries wherever available) to be equivalent to an AIS 4+ injury in humans (AAAM, 2008), the risk curves for CSDM and MPS were derived and then scaled to AIS 1+, 2+, 3+, and 5+ using ratios between the risk curves similar to those developed for HIC at 50% risk (NHTSA, 1995). These scaled CSDM and MPS risk curves represent various severities of concussive and hemorrhagic brain injuries. For example, AIS 3+ risk curve is a risk of severe concussion with the loss of consciousness 1-6 hours (AAAM, 2008), while AIS 4+ risk curve is for the loss of consciousness lasting over 6 hours. Finally, kinematic brain injury criterion (BrIC) was developed and applied to each test dummy (Hybrid III 50th male, Hybrid III 5th female, THOR 50th male, ES-2re, SID-IIIs, WorldSID 50th male, and WorldSID 5th female) as well as human volunteers based on college football data (Rowson et al., 2009, 2012).

The following hypotheses were tested in this study:

1. BrIC correlates best to both - CSDM and MPS, and rotational velocity (not rotational acceleration) is the mechanism for anatomic brain injuries.

2. The critical values for angular velocity are directionally dependent, and are independent of the ATD used for measuring them.

METHODS

Comparison of the SIMon and GHBMC FE Head Models

The SIMon and GHBMC human head models were tested using available experimental animal injury data, including rhesus monkeys (Abel et al., 1978; Stalnaker et al., 1977), baboons (Stalnaker et al., 1977), and miniature pigs (Meaney et al., 1993). A total of 67 animal brain injury experiments were simulated in the development of the biomechanical injury metrics – CSDM and MPS. The experimental kinematic loading conditions were scaled in amplitude and time to satisfy the equal stress/velocity scaling relationship, i.e., translational velocity scaled as 1, angular velocity as $1/\lambda$, and time scaled as λ , where λ is the scaling ratio (Takhounts et al., 2003). Once correctly scaled, these loading conditions were applied to the SIMon and GHBMC models. The SIMon FE model consists of 42,500 nodes and 45,875 elements, of which 5153 are shell elements (3790 rigid), 14 are beam elements, and 40,708 are solid elements (Takhounts et al., 2008). Major parts of the brain were represented: cerebrum, cerebellum, brainstem, ventricles, combined CSF and pia arachnoid complex (PAC) layer, falx, tentorium, and parasagittal blood vessels (Figure 2).

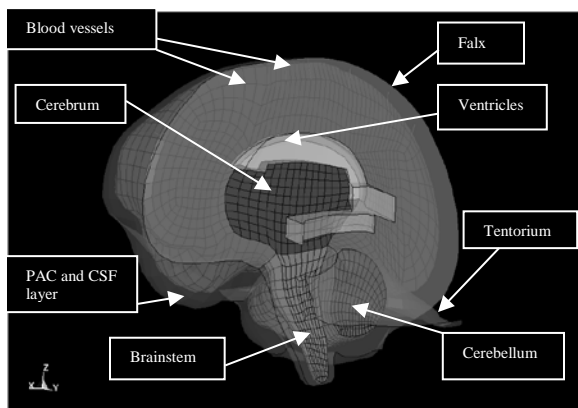


Figure 2. SIMon Finite Element Head Model.

The head of the GHBMC 50th percentile male human body model was extracted from the full body and used as part of this study. All image data used was acquired from a pre-screened individual who matched numerous anthropometric targets for the 50th percentile male (Gordon et al. 1989, Gayzik et al.

2012) within 5%. The subject selection and imaging protocol was approved by the Wake Forest University School of Medicine Institutional Review Board (IRB, #5705) [Gayzik 2009]. The participant's age, height and weight during enrollment were 26 years, 174.9 cm, and 78.6 ± 0.77 kg. Subject anthropometries pertinent to the head model were head breadth (16.4 cm), length (19.8 cm) and circumference (57.8 cm). The model consists of different anatomical structures of the brain including the cerebrum gray and white matter, corpus callosum, basal ganglia, thalamus, brainstem, cerebellum, and lateral and third ventricles (Figure 3), as well as cerebrospinal fluid (CSF), dural membranes, bridging veins, skull, facial bones, head flesh and head skin. The head model weighs 4.4 kg consisting of 270,787 elements with over 211,000 of which are solid elements.

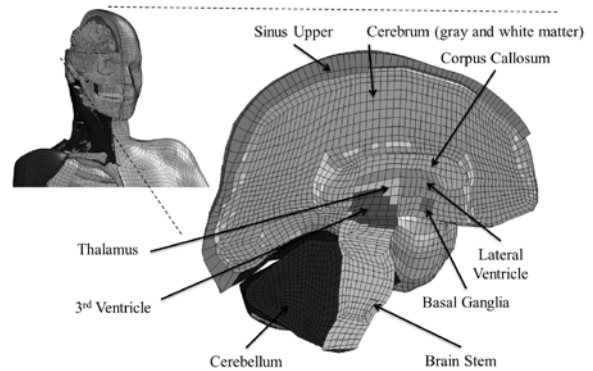


Figure 3. GHBMC v 3.5 head model, shown with full body model, parts labeled.

Both - SIMon and GHBMC head models were validated using the following tests: pressure was validated against a series of cadaveric intracranial pressure data reported by Nahum et al. (1977) and Trosseille et al. (1992). Brain motion with respect to the skull was validated against experimentally measured data from cadavers due to sagittal, coronal, and horizontal blunt head impacts performed by Hardy et al. (2001, 2007). Validation of the SIMon model is given in Takhounts et al. (2008), and that of the GHBMC model – in Mao et al. (2013). In addition, dynamic responses of the facial bone at various regions of GHBMC model were validated against force-deformation curves from nasal impact (Nyquist et al., 1986), zygoma and maxilla impact (Allsop et al., 1988). The validations for the skull bones were performed for frontal angled impact, crown impact, and occipital impact reported by Yoganandan et al. (1995) and frontal horizontal impact reported by Hodgson et al. (1970).

To compare the response of the two models all the animal data referenced above and described in Takhounts et al. (2003, 2008) were run with both SIMon and GHBMC FE head models and the injury risk curves were developed using both models. The results of both models were compared using R^2 coefficient of determination.

Pendulum Tests to Correlate Physical and Kinematic Parameters

Next, it was necessary to establish a relationship between physical injury metrics – CSDM, maximum pressure and MPS – with kinematic parameters, such as linear and angular head accelerations and velocities. For this purpose, a series of pendulum tests at various impact angles and energies were conducted on several ATDs – Hybrid III 50th male, Hybrid III 5th female, THOR 50th male, ES-2re, SID-IIs, WorldSID 50th male, and WorldSID 5th female. These tests were conducted using a hydraulic linear impactor (23.4 kg projectile mass with 4 inch diameter spherical impactor face) with impact speeds designed to generate HIC15 values ranging from 200 to 1800 in both padded and unpadded conditions. For the padded condition a one inch thick piece of gray “Ensolute SCC” foam was affixed to the head at the impact location. The height of the impact location was at the level where the nose bridge meets the forehead or an equivalent relative height with respect to the head for dummies without a nose (Figure 4).

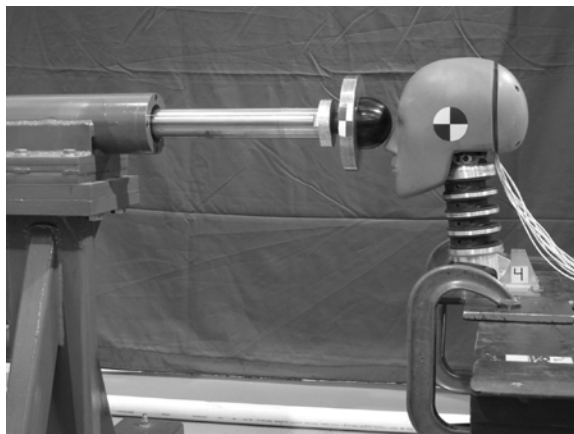


Figure 4. Pendulum test setup. The head and neck assembly of the HIII 50th percentile male ATD is shown for a frontal (0 degrees), unpadded impact at the head center of gravity.

The line of contact force was directed through the impact height at 0 or 30 degrees relative to the midsagittal plane for frontal impact dummies, and 60 or 90 degrees relative to the midsagittal plane for side

impact dummies. The wait time between consecutive tests on any particular head was 1 hour to allow for recovery of the soft materials. Overall 190 tests were conducted on all ATDs and then simulated with both FE models – SIMon and GHBMC to test the first hypothesis.

Correlations between physical and kinematic parameters were assessed using R^2 coefficient of determination, root mean square error (RMSE), and Coefficient of Variation (CV) defined as RMSE normalized by the mean of the dependent variable. The CV was used to compare the goodness of fit between the MPS data for which regression through the origin (RTO) formulation was used and CSDM data for which the ordinary least square (OLS) model was applied (Eisenhauer, 2003). This was necessary due to different formulations used by RTO and OLS to compute R^2 :

$$R^2 = \frac{\sum(\hat{Y}_i - \bar{Y})^2}{\sum(Y_i - \bar{Y})^2} = 1 - \frac{\sum(Y_i - \hat{Y}_i)^2}{\sum(Y_i - \bar{Y})^2}, \text{ for OLS}$$

$$R^2 = \frac{\sum \hat{Y}_i^2}{\sum Y_i^2}, \text{ for RTO,}$$

where Y_i is the i^{th} dependent variable (or value), \hat{Y}_i is the i^{th} fitted value, and \bar{Y} is the mean of the dependent variable.

The equations above indicate that it is meaningless to compare R^2 values between CSDM and MPS based charts, and instead CV should be used (Eisenhauer, 2003). To compare the ATDs data within the MPS (e.g. max angular velocity versus MPS for each dummy) and CSDM (e.g. max angular velocity versus CSDM for each dummy) groups, both the R^2 coefficient of determination and CV were used. SAS software (SAS, Version 9.3, Cary, NC) was used to run regression (for both RTO & OLS) and obtain R^2 , RMSE, and CV values for all datasets.

Development and Scaling of Risk Curves

It was assumed that at the higher severity range of injury spectrum (AIS 4+) animal subjects would experience anatomic brain injuries similar to those that would be observed from a human under the equivalent loading conditions. The equivalent loading conditions are defined through the application of the equal stress equal velocity scaling relationship between animals and humans.

The risk curves for CSDM and MPS were constructed using survival analysis (Weibull distribution, left/right censored data):

$$\text{Injury Risk} = 1 - e^{-\left(\frac{\text{CSDM}}{\lambda}\right)^k}, \quad (1)$$

where λ is scale and k is shape parameter for Weibull distribution.

This injury risk curve (Eq. 1) would correspond to AIS 4+ brain injury according to the recently published AIS scale (AAAM, 2008) for anatomic brain injuries. To obtain other levels of the abbreviated injury scale, the risk curves for HIC were used (NHTSA, 1995), assuming equal severity ratios between corresponding risk curves for HIC and CSDM at 50% risks. For example, to obtain AIS 3+ risk curve for CSDM, the ratio (β_{34}) of AIS 3+/AIS 4+ risk curves at 50% for HIC was found, and then AIS4+ risk curve for CSDM at 50% was multiplied by this ratio to find 50% risk point for the AIS3+ CSDM:

$$\text{CSDM AIS 3+ (50\%)} = \beta_{34} * \text{CSDM AIS 4+ (50\%)}. \quad (2)$$

Using equations 1 and 2 together, the CSDM risk curve for AIS 3+ was found, while keeping the shape parameter k of the Weibull distribution constant. Other risk curves for CSDM were found in the similar fashion (Takhounts et al. 2011). Similar procedure was followed for scaling MPS risk curves.

Alternatively, crash data from NASS-CDS may also be used to develop relative differences between AIS 3+, AIS 4+, and AIS 5+ BrIC risk curves. For this purpose, the NASS-CDS frontal (GAD1='F') cases were investigated from 1997 to 2011 with known crash delta V (i.e., change in velocity), belted, age 15+ occupants seated in the driver's or right front passenger's position for model year 1998 or newer vehicles. Simple binary logistic regression was done to assess the association between delta V, occupant age, percent overlap (e.g., full frontal versus partial overlap), vehicle model year, and principal direction of force (PDOF) and the dependent outcomes of interest; AIS 3+, 4+ and 5+ anatomic brain injuries. Predictors with p values < 0.10 were retained for use in creating a multivariable model using stepwise logistic regression. Using weighted data, three sets of AIS 3+, 4+, and 5+ risk curves were produced for anatomic brain injuries. The first was based on the injuries as coded in AIS 1998 (AAAM, 1998). The next two sets were based on AIS 2008 coding (AAAM, 2008). To accomplish this using injuries coded in NASS-CDS using AIS 1998, injuries that

have direct one-to-one coding or severity level changes between AIS 1998 and AIS 2008 were adjusted appropriately. Where there had been one code (e.g., 140652.4 – cerebrum hematoma, subdural, small) in AIS 1998 that is now represented by two codes in AIS 2008 (140652.4 and 140651.3 for “small” and now “tiny” subdural) both a “low” and “high” estimate was done. The “low” estimate took all such one (AIS 1998)-to-many (AIS 2008) codes when translating from AIS 1998 to 2008 and assigned the lowest possible AIS score. In this case, all AIS 1998 coded small cerebrum subdurals that were coded as 140652.4 in AIS 1998 are coded as 140651.3 for AIS 2008. This same translation or recoding was done for all one code to many code scenarios. The “high” estimate on the other hand assigned the highest possible AIS severity code in making the translation from AIS 1998 to 2008, which in the example of the cerebrum subdural means retaining the 140652.4 code.

Development of BrIC

To test the second hypothesis, the test data from these pendulum impact tests was then combined with the available NCAP and frontal offset tests (223 NCAP and frontal offset tests) with 7 ATDs to develop BrIC for all ATDs. To do that, first, CSDM/MPS values were calculated for each test. This was accomplished by scaling the load curves for each ATD (based on the ATD's head geometry) using equal stress equal velocity scaling relationship and applying them to both head models – SIMON and GHBM. The best linear fit between CSDM and BrIC was obtained in the form of equation (3) using critical value of max resultant angular velocity ω_{cr} such that BrIC = 1 when CSDM = 0.49 (50% probability of AIS 4+). Similar process was used with the MPS in place of CSDM. Maximum resultant angular velocity was initially selected for BrIC_R (the letter R here stands for “resultant”) formulation as it was the best correlate to both – CSDM and MPS (see Appendix I).

$$\text{BrIC}_R = \frac{\omega_{max}}{\omega_{cr}}, \quad (3)$$

It was observed, however, that different critical values of maximum angular velocity were achieved when the models were exercised rotationally in different directions (rotation about X-, Y-, or Z-axis) using generated loading conditions similar to that shown in Figure 5.

This directional dependence of the critical angular velocity was incorporated into a new formulation for BrIC as shown in equation (4) below:

$$BrIC = \sqrt{\left(\frac{\omega_x}{\omega_{xC}}\right)^2 + \left(\frac{\omega_y}{\omega_{yC}}\right)^2 + \left(\frac{\omega_z}{\omega_{zC}}\right)^2}, \quad (4)$$

where ω_x , ω_y , and ω_z are maximum angular velocities about X-, Y-, and Z-axes respectively, and ω_{xC} , ω_{yC} , and ω_{zC} are the critical angular velocities in their respective directions. Two approaches to calculate maximum angular velocities were investigated – (1) maxima in each direction irrespective of time the maxima have occurred; and (2) values in each direction at the time that the max x-, y- or z-component of angular velocity contributes most to BrIC (i.e. the component values at the time at which the max ω/ω_c occurs). Correlations between BrIC_R (equation 3) and CSDM/MPS for all ATDs combined, and between BrIC (equation 4) and CSDM/MPS for all ATDs combined were then compared using R^2 and CV.

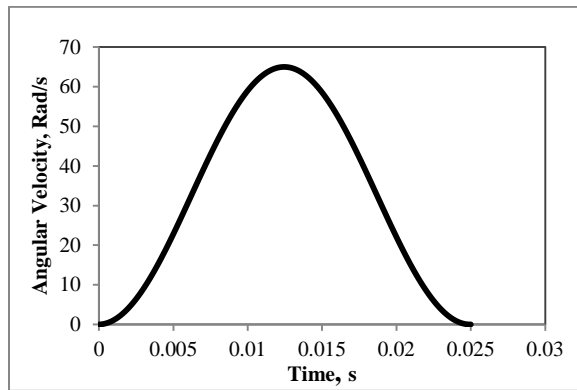


Figure 5. Loading curve for the models in each direction. Note: The span and magnitudes of the curve were altered to generate various magnitudes of CSDM and MPS.

Similarly to the procedure above, BrIC was evaluated based on translational and rotational data obtained from the college football players. Between 2007 and 2008, the helmets of 19 Virginia Tech football players were instrumented with a custom 6 degree of freedom (6DOF) head acceleration measurement device (Rowson et al, 2009). The measurement device consisted of 12 accelerometers and recorded linear and angular acceleration about each axis of the head using a novel algorithm (Chu et al, 2006). Any time an accelerometer exceeded 10 g during play, data acquisition was automatically triggered and data were collected for 40 ms (including 8 ms of pre-trigger data). Once data collection was complete, data were wirelessly transmitted to a computer on the sideline. Linear and angular head accelerations were recorded for a total of 4709 head impacts of which 362 had peak resultant linear accelerations greater

than 40 g. To determine resultant angular velocity, angular acceleration about each individual axis of the head was numerically integrated throughout the entire acceleration trace. Resultant angular velocity was then calculated. Each impact was visually inspected so that the angular acceleration (and resulting angular velocity) pulse of interest could be examined and peak values identified. Once peak angular acceleration and peak angular velocity were determined for each impact, a linear regression analysis was performed using a least squares technique. The regression model was constrained so that an angular acceleration of 0 rad/s² resulted in an angular velocity of 0 rad/s. Although none of the 6 DOF impacts resulted in brain or other head injury, CSDM and BrIC curves were computed to assess the potential for TBI.

Similar to above, concussive data was obtained from college football players using the commercially available 5 DOF HIT System (Simbex, Lebanon, NH). This head acceleration device consisted of 6 accelerometers and measure resultant linear acceleration of the head. This device is limited in that only peak angular acceleration can be estimated from an assumed pivot point in the neck. Resultant angular velocities for concussive data points were estimated from resultant angular accelerations using a regression model. Details of the methods used for data collection can be found in the literature (Duma et al, 2005, Duma et al, 2009). Using the HIT System, head acceleration data were recorded for 6 concussions between 2003 and 2008 (Duma et al, 2009). These 6 concussions were combined with concussive data collected from published studies that utilized identical data collection methods (Broglia et al, 2010, Guskiewicz et al, 2007). This resulted in a dataset of 32 concussions. Using this data, Rowson et al. (2012) constructed injury risk curves for concussion using rotational acceleration and rotational velocity as independent variables.

RESULTS

Comparison of the SIMon and GHBMC FE Head Models

Figures 6 and 7 demonstrate the correlation between results of GHBMC and SIMon models for CSDM and MPS using animal tests. Pendulum tests show similar high correlation between results of the two models. Figure 8 shows the receiver-operator characteristic (ROC) curve for both models using CSDM (0.25) as the injury criterion. The value of 0.25 in parenthesis indicates the strain threshold for computing CSDM (Takhounts et al. 2008). The SIMon model had an area under the ROC curve equal

to 0.83 while the GHBMCM model was slightly better at 0.86. Using MPS as an injury criterion reduced the area under the ROC curve to 0.78 for both models (Figure 9). It should be noted that these values of area under ROC curves are not the maximum obtainable values for CSDM (Appendix 0, Figure 0.1). For example, strain threshold of 0.10 gave the highest value of the area under ROC curve (0.89) when these strain thresholds were varied from 0.10 to 0.30 with 0.05 intervals. In choosing the strain threshold of 0.25 for CSDM calculations, area under ROC curves as well as a set of statistical fit parameters for risk curves evaluation, were considered. Statistical fit parameters were best for strain thresholds of 0.25 and 0.30 (Appendix 0, Figures 0.2 - 0.6) that degraded sharply for smaller and higher strain thresholds. Hence, the strain threshold of 0.25 was chosen for calculation of CSDM, which was the best compromise between the area under the ROC curve and statistical fit parameters.

The risk curves for CSDM are given in Figure 10 and for MPS – in Figure 11. The CSDM value that maximized sensitivity and specificity was equal to 0.65, which corresponded to approximately 69% risk in Figure 10. The MPS value that maximized sensitivity and specificity was equal to 0.97, which corresponded to approximately 55% risk in Figure 11. While CSDM had better ROC for both models and smaller error range for the Weibull shape parameter (Table 1), MPS had better risk curves as measured by the confidence intervals (Figure 11), and its value that maximized the sensitivity and specificity was closer to 50% risk. Max Log Likelihood and the error ranges in the Weibull scale parameters (Table 1) were comparable between the two measures with slight variations depending on the model.

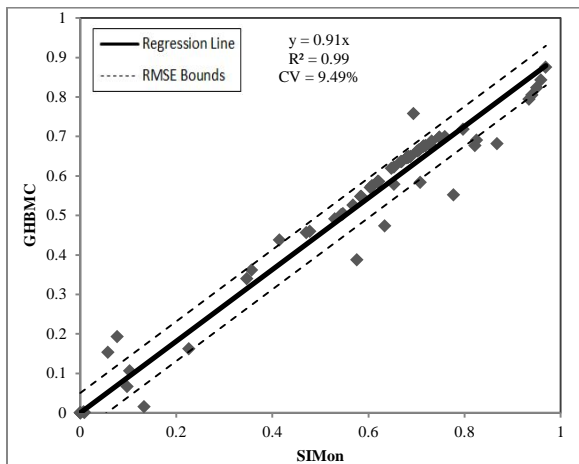


Figure 6. Comparison of CSDMs in animal tests between GHBMCM and SIMon models.

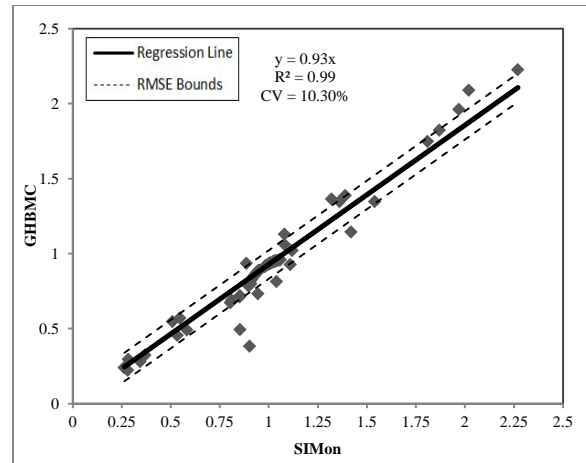


Figure 7. Comparison of MPSs in animal tests between GHBMCM and SIMon models.

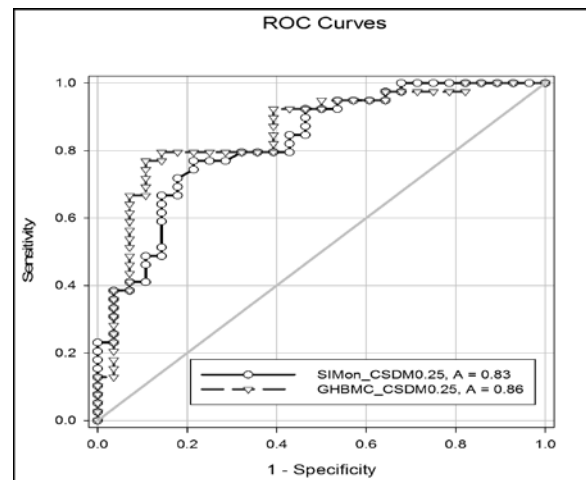


Figure 8. ROC curves for CSDM in animal tests for GHBMCM and SIMon models.

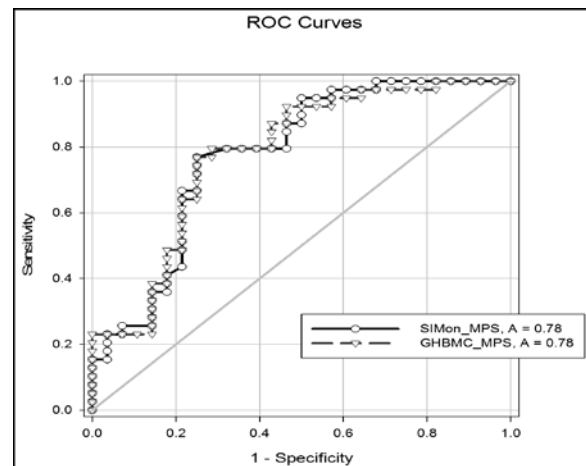


Figure 9. ROC curves for MPS in animal tests for GHBMCM and SIMon models.

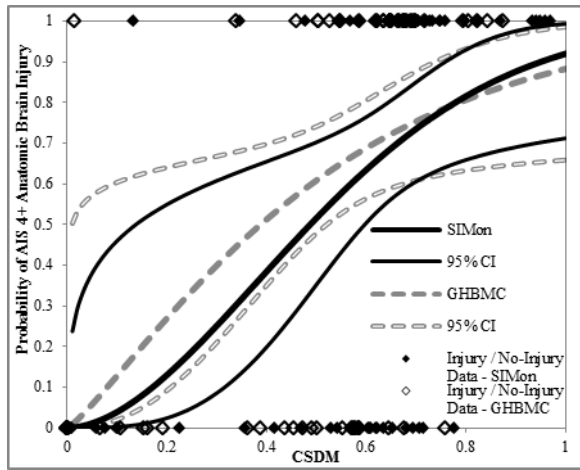


Figure 10. Risk of AIS 4+ anatomic brain injuries in animal tests as a function of CSDM.

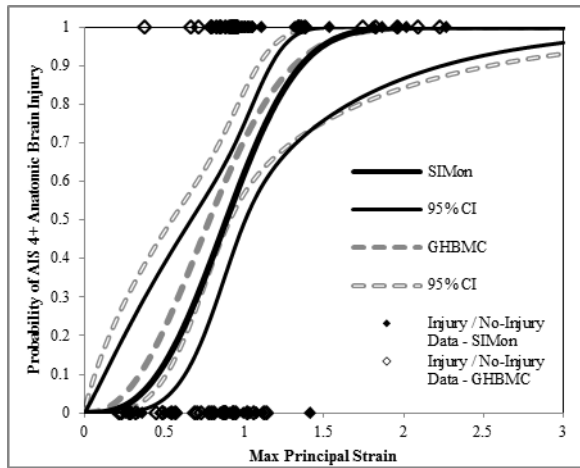


Figure 11. Risk of AIS 4+ anatomic brain injuries in animal tests as a function of MPS.

Table 1. Weibull parameters for CSDM and MPS for GHBM and SIMon models along with the standard errors (in parentheses) and Max Log Likelihood.

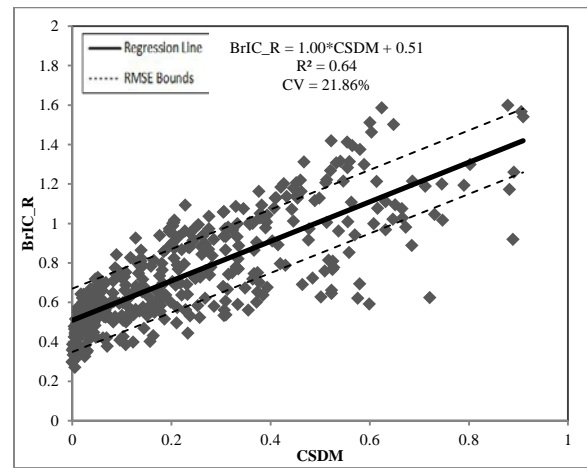
Case	Max LL	Weibull Scale (Std Error)	Weibull Shape (Std Error)
GHBM-CSDM	-36.88	0.53 (0.08)	1.19 (0.55)
SIMon-CSDM	-34.26	0.60 (0.06)	1.80 (0.74)
GHBM-MPS	-35.90	0.92 (0.07)	2.32(0.74)
SIMon-MPS	-34.90	1.01 (0.06)	2.84 (0.89)

Pendulum Tests to Correlate Physical and Kinematic Parameters

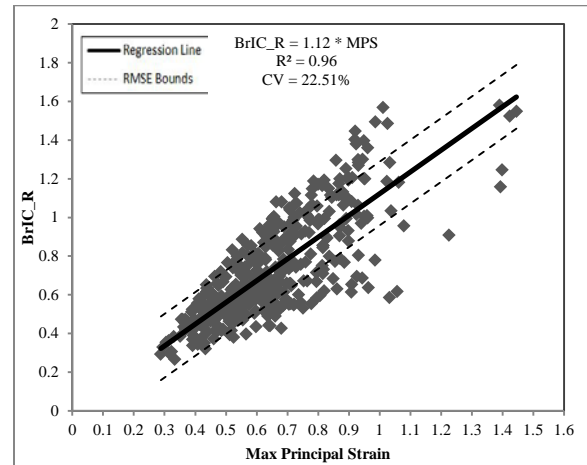
Correlations of physical (max pressure, CSDM, and max principal strain) and kinematic parameters (HIC15, max resultant linear acceleration, max

resultant angular acceleration, and max resultant angular velocity) for each dummy in pendulum tests are given in Appendix I (Figures I.1 through I.12). Max pressure correlated best with max resultant linear acceleration ($R^2 = 0.97$, CV = 18.85%, Figure I.2). CSDM correlated best with max resultant angular velocity ($R^2 = 0.91$, CV = 28.26%, Figure I.8). MPS correlated best with max resultant angular velocity ($R^2 = 0.98$, CV = 14.39%, Figure I.12). The R^2 and CV values above are given when the data from all dummies is lumped together.

The correlation between physical and kinematic parameters was reduced when NCAP and frontal offset data was added as shown in Figure 12 and Table 2 below.



(a)



(b)

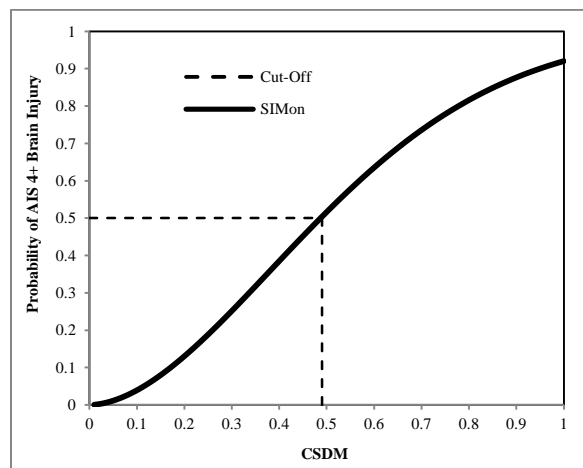
Figure 12. Correlation between (a) BrIC_R and CSDM and (b) BrIC_R and MPS for all dummies in available tests (413 data points) where BrIC was constructed using equation 3.

Table 2. Calculated critical angular velocities using equation 3 for each dummy and combined for all dummies.

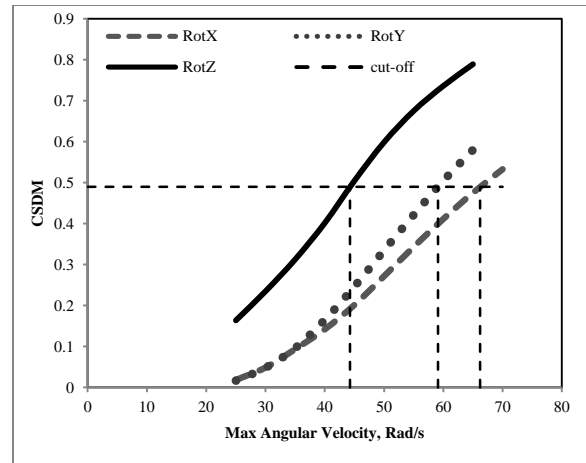
Dummy/ Human/ (All Available Tests)	Critical Max Resultant Angular Velocity Based on CSDM, Rad/s	R ² (CV %) BrIC_R vs CSDM	Critical Max Resultant Angular Velocity Based on MPS, Rad/s	R ² (CV %) BrIC_R vs MPS
HIII-50	57.96 ± 5.68	0.65 (17.47)	53.35 ± 6.88	0.96 (21.15)
HIII-5	54.41 ± 5.98	0.84 (13.18)	54.54 ± 6.86	0.98 (15.08)
THOR	44.35 ± 6.24	0.69 (16.81)	47.59 ± 7.51	0.96 (20.24)
ES2	50.09 ± 10.15	0.48 (26.29)	50.62 ± 10.94	0.93 (28.33)
SID-IIIs	62.44 ± 6.71	0.72 (16.99)	59.23 ± 5.77	0.98 (14.59)
WS-50	65.34 ± 4.61	0.78 (8.41)	67.38 ± 3.95	1.00 (7.20)
WS-5	69.63 ± 4.05	0.89 (6.24)	68.4 ± 5.55	0.99 (8.56)
VT- Football	45.18 ± 4.91	0.82 (20.15)	37.19 ± 2.06	0.99 (8.44)
Combined	54.19 ± 8.74	0.64 (21.86)	54.85 ± 9.00	0.96 (22.51)

Development of BrIC

The directional CSDM versus max angular velocity curves for the loading conditions shown in Figure 5 of the Methods section are given in Figure 13 b) below, where critical max angular velocity for each direction was calculated such that it corresponded to 50% probability of AIS 4+ anatomic brain injuries (this corresponded to CSDM = 0.49 in the SIMon model as shown in Figure 13 a)). Similar procedure was followed to find MPS based critical max angular velocities in each direction, where MPS = 0.89 in the SIMon model corresponded to 50% probability of AIS 4+ anatomic brain injuries.



(a)



(b)

Figure 13. a) Risk of AIS 4+ anatomic brain injury versus CSDM from SIMon model with the cut-off at 50% risk corresponding to CSDM value of 0.49; b) CSDM versus max angular velocity relationships demonstrating that the same risk (at CSDM = 0.49) is achieved at different max angular velocities in different directions.

Critical max angular velocities for each direction are given in Table 3.

Table 3. Critical max angular velocities in each direction based on CSDM, MPS, and their average. Note: the values are the same for all ATDs (and humans).

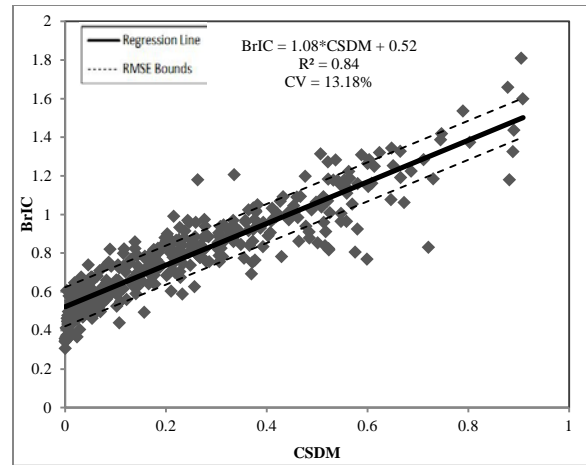
Critical Max Angular Velocity	Rad/s (CSDM Based)	Rad/s (MPS Based)	Rad/s (Average of CSDM and MPS)
ω_x	66.20	66.30	66.25
ω_y	59.10	53.80	56.45
ω_z	44.25	41.50	42.87

These critical max angular velocities were then evaluated for each tested dummy in both – pendulum tests described above and the available NCAP and frontal offset tests (those equipped with either nine accelerometer array or angular rate sensors). Using the CSDM based critical angular velocities given in Table 3 the critical values for BrIC at CSDM of 0.49 (50% probability of AIS 4+ anatomic brain injury) were computed to assess the possible error (e.g. how much the calculated critical BrIC value deviated from the value of 1.0). Similar procedure was followed for MPS. To reconcile the difference between CSDM based and MPS based critical angular velocity values,

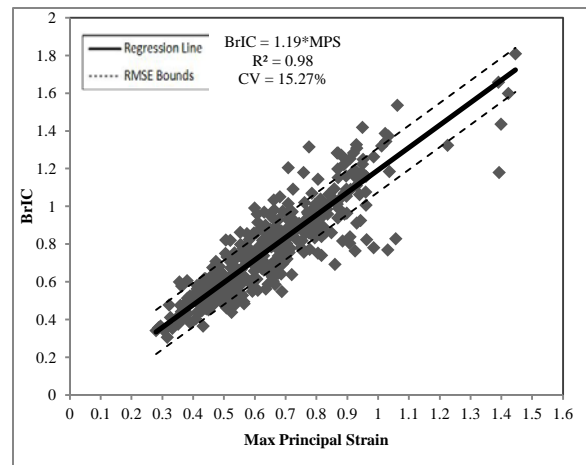
the average was taken and critical value of BrIC was also evaluated for both CSDM and MPS datasets based on these average values. Table 4 lists these BrIC values for each ATD (and humans from the college football players dataset) and for all the ATDs combined. The difference between 1.0 and the values in BrIC columns of Table 4 for each ATD gives an error associated with the use of the same critical values of angular velocities. For example, the CSDM based BrIC values for THOR, ES2 and Human are equal to 1.0 (zero error), while those for SID-IIs and WS-5 are 1.14 and 1.12 giving 14% and 12% errors respectively. For all ATDs combined this error is 5% for CSDM based BrIC (last row, BrIC = 1.05), and 6% for MPS based BrIC (last row, BrIC = 1.06). Figure 14 (a) shows the correlation between BrIC and CSDM, while Figure 14 (b) shows the correlation between BrIC and MPS. Note: the first approach in calculating BrIC was adapted where max angular velocity in each direction was calculated irrespective of the time it has occurred as the second approach did not improve the correlation between BrIC and CSDM (and MPS).

Table 4. Calculated BrIC values for each dummy and combined for all ATDs (and humans).

ATD	BrIC (Average critical values, CSDM dataset)	R ² (CV %) (Average critical values, CSDM dataset)	BrIC (Average critical values, MPS dataset)	R ² (CV %) (Average critical values, MPS dataset)
HIII-50th	1.09	0.73 (13.86)	1.03	0.97 (17.95)
HIII-5th	1.08	0.88 (12.30)	1.08	0.98 (14.75)
THOR	1.00	0.80 (15.99)	1.05	0.97 (19.09)
ES2	1.00	0.75 (13.73)	1.04	0.98 (16.11)
SID-IIs	1.14	0.92 (7.37)	1.10	0.99 (7.83)
WS-50	1.05	0.83 (7.10)	1.09	1.00 (5.40)
WS-5	1.12	0.98 (2.10)	1.10	1.00 (4.54)
Human	1.00	0.85 (19.63)	0.80	1.00 (7.44)
All ATDs	1.05	0.84 (13.18)	1.06	0.98 (15.27)



(a)



(b)

Figure 14. Correlation between (a) BrIC and CSDM and (b) BrIC and MPS for all dummies in available tests (413 data points) using formulation given in equation 4.

Development and Scaling of Risk Curves

The ratios β_{i4} , where i is the level of AIS of interest based on equation 2, are given in Table 5 (reproduced from Takhounts et al., 2011).

Table 5. Ratios for computing risk curves for AIS1+, 2+, 3+, and 5+ based on known risk curve for AIS4+.

β_{14}	β_{24}	β_{34}	β_{54}
0.10	0.50	0.82	1.04

Using alternative method for calculating coefficients β where NASS-CDS data was used, three sets of models associated respectively with AIS 3+, 4+, and

5+ anatomic brain injuries were produced. In all cases, occupant age, delta V, and percent overlap were included in the models. Vehicle model year and PDOF were not found to be significant predictors of AIS 3+, 4+ or 5+ brain injuries. Table 6 lists the model coefficients and the area under the ROC curve for the respective models. Note the area under the ROC curve in all cases had values of 0.81 or greater.

Table 6. AIS 3+, 4+, and 5+ Anatomic Brain Injury Risk Models – Frontal Crashes, NASS-CDS.

	Model	Model Coefficients				ROC Curve (area under)
		Intercept	DV	Age	Overlap	
AIS 1998	AIS3+	-7.0798	0.0619	0.0258	-0.0254	0.87
	AIS4+	-6.6144	0.0522	0.0205	-0.0291	0.87
	AIS5+	-11.837	0.0975	0.0394	-0.0131	0.82
AIS 2008 - Low	AIS3+	-7.0798	0.0619	0.0258	-0.0254	0.87
	AIS4+	-6.611	0.0525	0.0204	-0.0292	0.87
	AIS5+	-11.689	0.0974	0.0387	-0.0144	0.82
AIS 2008 - High	AIS3+	-6.8694	0.0581	0.0247	-0.0253	0.87
	AIS4+	-6.1674	0.041	0.0195	-0.0315	0.84
	AIS5+	-11.454	0.0925	0.0427	-0.0191	0.81

The models from Table 6 allow for estimates of the difference in risk of AIS 3+, 4+ and 5+ anatomic brain injury given a set of values of delta V, occupant age, and percent overlap. For example, if age is set to 45 or roughly the average of the driving population, and delta V and percent overlap values are representative of a frontal New Car Assessment Program (NCAP) test at 60 kph and 100%, respectively. The resulting AIS 3+, 4+ and 5+ percent risk of anatomic brain injury is predicted to be 0.86%, 0.4% and 0.42%, respectively, based on AIS 1998 models. The average age, delta V, and percent overlap of the AIS 3+ anatomic brain injury cases was 48 years, 53 kph, 55%, respectively. The AIS 3+, 4+ and 5+ predicted risk using these average values was 1.9%, 1.1% and 0.4%, respectively

Table 7 compares the current AIS 3+, 4+, and 5+ differences in risk as estimated at the average age, delta V, and percent overlap values noted above versus the 50% risk values from the expanded HIC curves used by Takhounts et al. (2011) and the expanded Prasad-Mertz HIC curves previously described by NHTSA (NHTSA, 1995). It can be seen that the percent difference varies significantly depending on the method chosen with the ratio of AIS 4+ to 3+ injury ranging from roughly 0.4 to 0.8.

Table 7. Ratios for expanding respective AIS 3+, 4+, 5+ Injury Risk Curves.

Curve Expansion Method	Ratio - AIS 4+ to 2+	Ratio - AIS 4+ to 3+	Ratio - AIS 4+ to 5+
Current NASS-CDS Regression Models - AIS 1998	NA	0.61	2.79
Current NASS-CDS Regression Models - AIS 2008, Low	NA	0.61	2.72
Current NASS-CDS Regression Models - AIS 2008, High	NA	0.46	2.13
Takhounts et al. (2011) - Expanded HIC	0.5	0.82	1.04
NHTSA - Expanded Prasad-Mertz HIC	0.41	0.67	1.29

The risk curves for CSDM, MPS and BrIC below are scaled based on the same ratios as in Takhounts et al. (2011) given in Table 5. However, other expansions given in Table 7 may also be utilized.

To construct a risk curve for CSDM based on SIMon model one would have to use equation 1 along with the data given in the second row of Table 1 (this risk curve is given in Figure 10 for AIS 4+ anatomic brain injuries). Figure 15 gives the set of risk curves for CSDM, where AIS 1+, 2+, 3+, and 5+ risk curves were obtained by scaling the AIS 4+ risk curve at a level of 50% probability of injury using coefficients from Table 5. Similar procedure was used to obtain risk curves based on MPS (Figure 16).

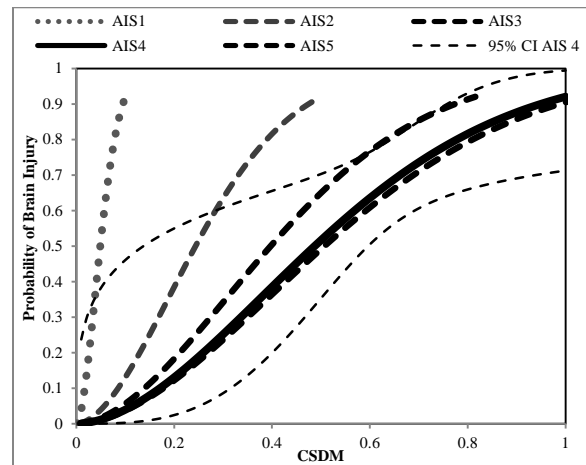


Figure 15. CSDM based risk of brain injuries for various severities.

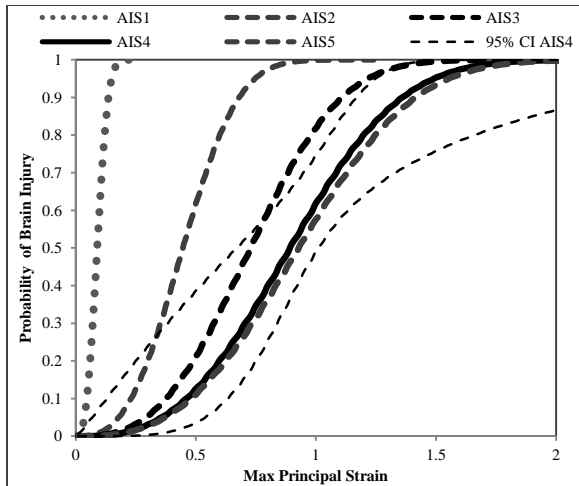


Figure 16. MPS based risk of brain injuries for various severities.

The CSDM and MPS based BrIC risk curves for AIS 4+ anatomic brain injuries were then obtained from the linear relationships between CSDM – BrIC/BrIC_R, and MPS – BrIC/BrIC_R respectively. AIS 5+, 3+, 2+ and 1+ are obtained in the manner similar to CSDM described above. Figures 17 and 19 show the “Combined” (Table 2) BrIC_R risk curves with the use of Figure 12 and Equation 3. Figures 18 and 20 give the “All ATDs” (Table 4) BrIC risk curves with the use of Figure 14 and Equation 4. Appendix III gives equations for all the risk curves in Figures 15 – 20 (Tables III.1 – III.6).

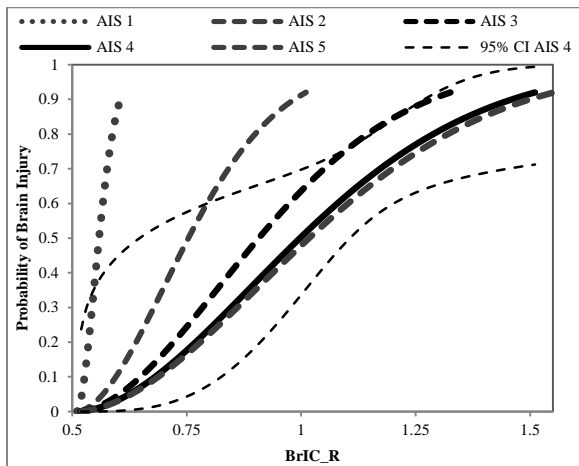


Figure 17. BrIC_R based on CSDM and formulation given by equation 3.

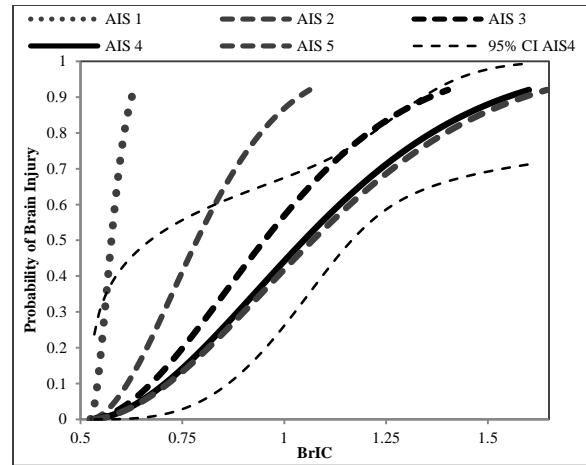


Figure 18. BrIC based on CSDM and formulation given by equation 4 (average critical angular velocities from Table 3).

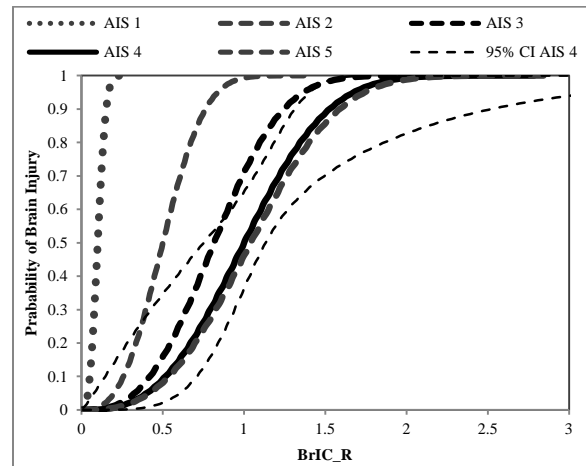


Figure 19. BrIC_R based on MPS and formulation given by equation 3.

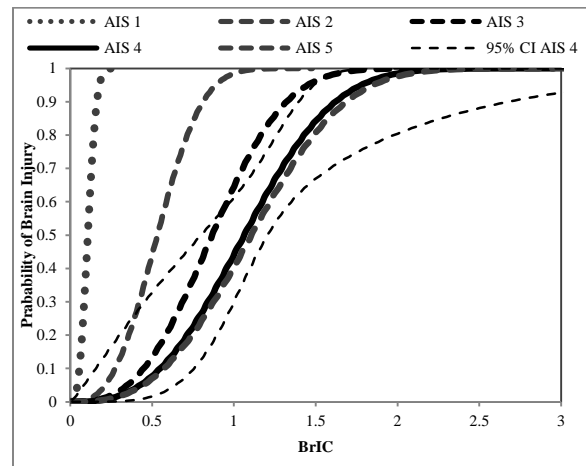


Figure 20. BrIC based on MPS and formulation given by equation 4 (average critical angular velocities from Table 3).

DISCUSSION

The importance of head rotational kinematics as a mechanism for brain injuries has been discussed in the scientific literature since the 1940s (Holbourn, 1943, Gennarelli et al. 1972, Ueno and Melvin 1995). More recently, Hardy et al. 2001 and 2007, in the experiments describing the motion of brain with respect to the overall motion of the skull, noted that angular velocity was the most “convenient” measure in describing relationship between brain and skull kinematics. Takhounts et al (2008) described that one of the ways to deform/strain a soft, nearly incompressible material (brain) contained within an almost undeformable shell (skull) is to rotate the shell.

Despite the overwhelming evidence of the head rotational kinematics to be a mechanism for brain injuries, the difficulty was in relating animal injury data (Abel et al. 1978; Gennarelli et al. 1982; Stalnaker et al. 1977; Nusholtz et al. 1984; Stalnaker et al. 1977; Meaney et al. 1993, Ommaya, 1985) to the potential for brain injuries in humans. One way to accomplish this is to find injury criteria for animals and scale it to humans using various scaling relationships (Ommaya, 1985). The advantage of this approach is in its simplicity – it is straightforward and a criterion is easily computed. The disadvantage of the approach is also in its simplicity as it doesn’t necessarily address the equivalency of the brain deformations (believed to be the primary cause of TBI) inside the brains of animals and humans. Another approach for relating animal injury data to humans is to develop FE models of animals and humans, find a scaling relationship between the two (Takhounts et al, 2003), and then develop a deformation/strain based criterion (CSDM or MPS) that would be equally applicable for both animals and humans. The advantage of this approach is that it gives a link between deformation fields inside the brains of animals and humans and thus may be more physically/biomechanically justifiable. Also, this approach allows for introduction of new information/data in addition to animal injury data, e.g. human data on brain material properties, brain deformations data – neutral density target data, pressure data, college football data, etc. This new information not only allows for establishing of the mechanisms of brain injury, but also synthesizes all the available information into one, physically meaningful criterion. The disadvantage of the approach is that it requires a powerful computer and several hours of run time to calculate CSDM and/or MPS. Both approaches, however, suffer from the lack of knowledge of how the injury severity in animals

would translate to the injury severity in humans given equivalent loading conditions.

The second approach was adapted in this paper where already developed and validated finite element models of human head – SIMon and GHBMC – were employed along with the injury criteria for DAI – CSDM and/or MPS. It should be noted that the term “DAI” used in this paper is a generic term for a severe anatomic brain injury in the animal data. In some cases it just corresponded to AIS 4+ brain injury (no skull fracture), in others it corresponded to a “severe concussion” in animals expressed in the length of unconsciousness (over 15 minutes for miniature pigs and monkeys), or “severe hematoma”. It is assumed that at the equivalent severity level of anatomic brain injury (AIS 4+) between humans and animals, the equivalent kinetic inputs necessary to produce these injuries in both species will scale according to the equal stress equal velocity scaling relationship (see Takhounts et al., 2003 and 2008 for detail on scaling). This is the only “inter-species” assumption made herein, as opposed to Takhounts et al. (2003) where individual injury types in the animals (DAI, acute subdural hematomas, focal lesion, etc.) were linked to similar injury types in humans using the same scaling relationship. In other words, the current approach assumes that the relationship between anatomic brain injuries in humans and animals exists at the rather high end of the severity spectrum, e.g. AIS 4+. The advantage of this assumption is that once the “link” between humans and animals is given, the other levels of severity (AIS 1+, 2+, 3+, and 5+) for humans may be derived by other means that will involve only human data (intra-species scaling). Different approaches to accomplish this are given below when the severity scaling is discussed.

The same animal data was used to compare the CSDM and MPS computed by the two head models – SIMon and GHBMC. As figures 6 and 7 illustrate, CSDMs computed using SIMon and GHBMC correlated to each other with $R^2 = 0.99$ (CV = 9.49%), while MPSs correlated to each other with the $R^2 = 0.99$ (CV = 10.30%) (Figures 6 and 7). The area under the ROC curve for CSDM using SIMon model was 0.83 while it was slightly higher (0.86) when GHBMC model was used (Figure 8). The area under the ROC curve for MPS were equal to 0.78 for both models (Figure 9) indicating that CSDM may be a slightly better predictor of DAI in animal tests. However, when risk curves were built for CSDM and MPS, MPS had narrower confidence intervals (and a better shape) than CSDM for both models (Figures 10 and 11). The Max Log Likelihoods for both

models and injury measures (CSDM and MPS) were comparable (Table 1). Since there were no significant differences between the results of the two models all subsequent calculations were made using only SIMon model to save computer time and for the sake of consistency with the previous publications on the subject (Takhounts et al., 2003, 2008, and 2011). It should be noted, however, that only pressures, CSDM and MPS were compared between the two models, and since the resolution of the GHBMC head model is much greater than that of the SIMon model it is expected that the difference between the models may be more pronounced when local strains and stresses are investigated.

Next, it was necessary to establish relationship between the physical parameters (CSDM, MPS and max pressure) with the kinematic parameters: HIC15, max resultant linear acceleration, max resultant linear velocity, max resultant angular accelerations and max resultant angular velocity. Previously (Takhounts et al., 2011) this was done using available NCAP test data where good correlations was hard to establish due to limited range of impact severities. To fill this gap in impact severities, lab controlled pendulum impacts to the heads of various dummies at different impact locations and angles (padded and unpadded) were conducted, where impact severities were controlled by varying calculated HIC15 values (from 200 to 1,800). Appendix I demonstrates the relationships between CSDM, MPS, and max pressure with the kinematic parameters for all dummies combined. It is clear that both CSDM and MPS correlated best with the max resultant angular velocity with MPS having better correlation ($R^2 = 0.98$, $CV = 14.39\%$, Figure I.12) than CSDM ($R^2 = 0.91$, $CV = 28.26\%$, Figure I.8). Max pressure correlated better with the max resultant linear acceleration ($R^2 = 0.97$, $CV = 18.85\%$, Figure I.2) and HIC15 ($R^2 = 0.93$, $CV = 28.84\%$, Figure I.1). It is worthwhile noticing that max resultant angular acceleration didn't correlate to any physical parameter with CV values ranging from 42.61% for max pressure to 91.61% for CSDM.

Interesting observations were made regarding the correlation between CSDM and HIC15. As Figure I.5 of Appendix I illustrates, when the data from all the dummies are combined there is no correlation between the two variables ($R^2 = 0.08$, $CV = 88.23\%$). The test data from the HIII 50th male dummy was then further investigated (there were more data points for this dummy, and it was tested at more impact locations and angles, padded/unpadded). Figure II.1 of Appendix II shows the correlation between CSDM and HIC15 for all HIII 50th male pendulum dummy

tests. R^2 is only 0.22, and $CV = 114.63\%$. However, when each impact type was isolated where only impact severity was varied, the correlations between the two variables became very good (most R^2 are greater than 0.90, and CVs are substantially lower). For example, Figure II.2 demonstrates that for the padded pendulum impact at the head center of gravity with 0 degrees angle (basically straight impact to the nose) the correlation between CSDM and HIC15 is quite high ($R^2 = 0.92$, $CV = 17.78\%$). Similar values of the correlation coefficients were observed in all the other impact conditions (Figures II.3 -II.6) with the exception of the 30 degrees padded impacts at head CG (Figure II.7) where correlation coefficient was $R^2 = 0.25$ ($CV = 37.04\%$), "spoiled" by one test. This example demonstrates that for similar test conditions (impact angles, location, padding, etc.) there is high correlation between two seemingly different head/brain injury criteria – HIC and CSDM. Similarly, correlations between CSDM and max linear acceleration and even max angular acceleration were improved when restrained to a specific testing mode, although these correlations were not as good as the one with HIC.

Pendulum tests demonstrated that max resultant angular acceleration did not correlate to any physical parameter – CSDM, MPS, or max pressure, and hence should be excluded from the BrIC formulation described in Takhounts et al. (2011) and only max resultant angular velocity should be retained in the new formulation (equation 3). Furthermore, between the two physical parameters (CSDM and MPS), MPS correlated to max resultant angular velocity better ($R^2 = 0.98$, $CV = 14.39\%$) than CSDM ($R^2 = 0.91$, $CV = 28.26\%$). However, when NCAP and frontal offset test data were added to the pendulum tests, the correlation between max resultant angular velocity and CSDM dropped from 0.91 to 0.64 (CV improved from 28.26% to 21.86%, Figure 12 (a)), and with MPS from 0.98 to 0.96 (CV dropped from 14.39% to 22.51%, Figure 12 (b)). This drop in correlation was thought due to the mostly in plane motion of the head in pendulum impacts, while head motion in most NCAP and frontal offset tests were more complicated resulting in 3-dimensional head motion. This is important because there may be difference in tolerance levels of the brain (as expressed via CSDM and MPS) in different directions. This hypothesis was tested using BrIC formulation expressed by equation (4), where different critical values of angular velocities were derived for different directions using procedure described in the Introduction and Methods. Two approaches were used for calculating BrIC from equation (4): (1) max angular velocity in each direction was calculated irrespective of the time they

have occurred, and (2) the time of the max component of angular velocity that contributes to the BrIC the most was noted and the other two components calculated at that time. Using the first approach the correlation between BrIC and CSDM improved from 0.64 (CV = 21.86%) to 0.84 (CV = 13.18%) as shown in Figures 12(a) and 14 (a), and between BrIC and MPS from 0.96 (CV = 22.51%) to 0.98 (CV = 15.27%) as shown in Figures 12(b) and 14(b). The second approach did not improve this correlation, and the first approach was adapted where max angular velocity in each direction was calculated irrespective of the time it has occurred. There were two sets of the max critical angular velocity components – one is derived using CSDM, the other using MPS (Table 3). Although the trend is similar, e.g. both sets have the lowest value for z-direction and highest in x-direction, there are still differences nevertheless. To reconcile these differences, the average of the two critical values in each direction was also tested and the correlation between the BrIC and CSDM and BrIC and MPS did not change.

Next, scaling of the risk curves for CSDM and MPS from AIS 4+ up to AIS 5+ and down to AIS 3+, 2+ and 1+ was performed based on the process described in Takhounts et al. (2011). This process was based on the assumption that BrIC severity ratios would be similar to those derived for HIC (NHTSA, 1995) at a 50% probability of injury. There may be other ways to scale risk curves for different severities. One of them is to use NASS-CDS data to estimate the risk of anatomic brain injuries at various severities. This process is complicated, however, when “translating” AIS 1998 codes to the latest AIS 2008 codes for anatomic brain injuries resulting in two possible sets of scaling parameters (Table 7), especially for scaling from AIS4+ to AIS5+. Another observation is that the scaling ratios for AIS 4+ to AIS 3+ varied substantially depending on the method used. At one end of the range are the two HIC-based scaling ratios (last two rows in Table 7) with this ratio varying from 0.67 to 0.82, while NASS-CDS based method gave the range of 0.46 to 0.61 (first 3 rows of Table 7). It was decided to provide the risk curves based on the Takhounts et al. (2011) – the method based on the existing HIC ratios, for two reasons (although risk curves based on the other methods could also be obtained based on the information given within body of this paper): 1) NASS-CDS method did not provide a reliable scaling ratio for AIS 2+ (and AIS 1+) risk curve, which was used to relate to the concussion data (see discussion below); 2) ratio for calculating AIS 3+ risk curve based on the NASS-CDS method (rows 1-3 in Table 7) are smaller than that for AIS 2+ ratio based on HIC-scaling (row 4 in Table 8). That

said, the scaling ratios may not be final as the NASS-CDS method may be refined in the future, which is the subject of another, more in depth, research on the subject.

Once CSDM and MPS risk curves were obtained and scaled for various AIS levels (using the same method as in Takhounts et al., 2011), BrIC risk curves were obtained using formulations given by equations 3 (Figure 12) and 4 (Figure 14), where BrIC was set to the value of 1.0 to correspond to 50% probability of AIS 4+ injury. The risk curves for equation (3) formulation were necessary to compare with the previously published data for concussion in college football players (Rowson et al., 2012) and in scaled monkey data (Ommaya, 1985) as the resultant max angular velocity was used in these studies. However, it is recommended that the equation (4) based formulation of BrIC and the corresponding risk curves are used in the future as this formulation provides better correlation with both CSDM and MPS.

Rowson et al. (2012) gave a risk curve for concussions in college football players based on the max resultant angular velocity. Based on their estimate, 50% probability of concussions was at max resultant angular velocity value of 28.3 rad/s. Assuming that these concussions are represented by the AIS2+ risk curve (Figure 19), BrIC value at 50% probability of AIS2+ is 0.50. Since this risk curve was derived from combined dataset, the critical value for max resultant angular velocity for combined dataset is 54.85 rad/s (last row of Table 2 for MPS). Multiplying BrIC of 0.50 by the critical value of 54.85 rad/s will give the value of the max resultant angular velocity for the 50% probability of AIS2+ brain injury. This value is 27.43 rad/s, which is comparable to the similar risk of concussion in college football players.

Ommaya (1985) gave an overview of the rotational injury tolerance values for the onset of concussion based on the research conducted on rhesus monkeys and chimpanzees. The human rotational tolerances were obtained using a mass scaling relationship for angular accelerations (inversely proportional to the two-thirds power of the brain mass) giving angular velocity and acceleration tolerances for human of 20 – 30 rad/s and 1,800 rad/s² respectively. Inserting these tolerance values into equation (3) and using critical value for MPS from the last row of Table 2 will give BrIC values between 0.36 (for angular velocity of 20 rad/s) and 0.55 (for angular velocity of 30 rad/s). Referring to the AIS2+ risk curve for MPS (Figure 19) will give a risk of concussion ranging

from 25% - 59% depending on the chosen tolerance value of angular velocity.

In both examples above the formulation of BrIC based on MPS was chosen. This is due to the fact that BrIC and BrIC_R risk curves based on MPS (Figures 19 and 20) start at (0, 0) point while the BrIC and BrIC_R risk curves based on CSDM don't (Figures 17 and 18). This is due to the nature of CSDM calculation that starts at a non-zero value of angular velocity. Because of this feature of CSDM, it was deemed more appropriate to use MPS-derived risk curves for BrIC.

There are many limitations in this study, most of which have been discussed above. These are:

- First, all the limitations that were applicable in the development and validation of SIMon finite element head model (Takhounts et al, 2003, 2008) are applicable to this paper as well. In addition, correlation between CSDM/MPS and BrIC is not perfect and will add additional errors to the injury risk estimates. It should be noted, however, that similar limitations are applicable to any research – computational and/or experimental.
- Second, only DAI type anatomic brain injuries in animals were investigated in this study. Inclusion of other types of TBI, such as focal lesions, contusions, etc. may change the relationship for BrIC, especially at the lower severity of injury spectrum. However, BrIC is not an “ultimate” head injury criterion that captures all possible brain injuries and skull fractures, but rather a correlate to a subset of TBI with head rotation believed to be a primary injury mechanism.
- Third, deriving CSDM, MPS and BrIC risk curves for various AIS levels based on ratios between 50% risks for different AIS levels for HIC assumes that rotationally induced injury severities change proportionally to those induced translationally (which on their own may not be accurate – see other possible methods of deriving these ratios). This assumption may or may not be correct, but due to lack of any data on rotational based changes in injury severity this assumption provides a “first approximation” of these changes. Other methods of such severity scaling should be investigated in the future
- Fourth, although very valuable, the college football data has its own limitations: athletes are trained to sustain higher loads, the average concussed angular velocity and acceleration were calculated from the 5 DOF measuring system rather than measured directly by the 6 DOF system, thus the

accuracy of these values may be questioned. In addition, clinical assessment of concussion is not well standardized that may contribute to additional measuring errors.

- Fifth, regarding scaling of the animal tolerances to those of humans, it is interesting to give a quote from Ommaya (1985): “It should be reemphasized that this information (rotational tolerances) is considered to be reliable for the Rhesus, sketchy for the chimpanzee, and completely speculative for man.” He then suggests revising the human rotational tolerances when the data from accident reconstruction in humans become available. College football data may be considered as one of these “accident reconstruction” data.

- Finally, BrIC is a rotational injury criterion (see second limitation), while HIC is a translational injury criterion (calculated using translational accelerations only), and combining the two may better capture head injuries. However, a human head is rarely experiencing just rotational or just translational motion. It usually is experiencing both. Furthermore, when direct impact to the head is present, skull deformation may play a role in brain injuries (Nusholtz et al. 1984), especially for a younger population. This paper does not address this combination of both modes of motion (rotational and translational) and corresponding (combined) injury mechanisms. Neither does it address possible injuries due to skull deformation. These will have to be investigated in the future.

Despite the limitations that are inherent in any research, this paper provides valuable information on the importance of limiting rotational kinematics of the human head that may be beneficial to both – athletes and the general driving population.

It should be noted that the primary purpose of this manuscript was to present the development of BrIC and the associated injury risk functions. The value of BrIC = 1.0 is not proposed as an Injury Assessment Reference Value (IARV) at this time. More work is necessary before an IARV can be proposed. Among other things, this work includes reviewing the field data, simulating some of the cases from the field, examining potential countermeasures, and evaluating the benefits when a restraint system is optimized for BrIC alone, HIC alone, or BrIC and HIC combined.

CONCLUSIONS

Following are the conclusions of the paper:

- Two different validated human head/brain finite element models were used in the developments of BrIC – SIMon and GHBMC. Both models showed similar results.
- Angular velocity correlated to two physical parameters – CSDM and MPS, and is the only component of BrIC. Angular acceleration did not correlate well to any physical parameter and hence was excluded from the BrIC formulation.
- The critical values for angular velocity are directionally dependent, and are independent of the ATD used for measuring them.
- MPS based risk curves are recommended to use for BrIC based on the formulation given by equation (4) (Figure 20 and Table III.6 of Appendix III).

ACKNOWLEDGMENTS

The views and opinions expressed in this manuscript are those of the authors only and not necessarily of NHTSA. The authors would like to acknowledge Scott Gayzik of the Wake Forest University and Liying Zhang of the Wayne State University for their help with the GHBMC head model.

REFERENCES

- Allsop, D.L., C.Y. Warner, M.G. Wille, D.C. Scheider, and A.M. Nahum (1988) Facial impact response - A comparison of the Hybrid III dummy and human cadaver. In Proc. 32nd Stapp Car Crash Conference, SAE Paper No. 881719.
- Abbreviated Injury Scale 1990 Edition (1998 Update) Association for the Advancement of Automotive Medicine, Des Plaines, IL.
- Abbreviated Injury Scale 2005 (2008 Updated) Association for the Advancement of Automotive Medicine, Des Plaines, IL.
- Abel, J., Gennarelli, T.A., Seagawa, H. (1978) In cadence and severity of cerebral concussion in the rhesus monkey following sagittal plane angular acceleration. Proc. 22nd Stapp Car Crash Conference, pp. 33-53, Society of Automotive Engineers, Warrendale, PA.
- Bandak, F.A., and Eppinger, R.H. (1995) A three-dimensional finite element analysis of the human brain under combined rotational and translational acceleration. Proc. 38th Stapp Car Crash Conference, pp. 145-163. Society of Automotive Engineers, Warrendale, PA.
- Broglio, S.P., Schnebel, B., Sosnoff, J.J., Shin, S., Fend, X., He, X., and Zimmerman, J. (2010) Biomechanical properties of concussions in high school football. *Med Sci Sports Exerc*, 42(11): 2064-71.
- CDC, National Center for Injury Prevention and Control (2003) Traumatic Brain Injury Facts, <http://www.cdc.gov/ncipc/factsheets/tbi.htm>.
- Chu, J. J., Beckwith, J. G., Crisco, J. J., and Greenwald, R. (2006) A Novel Algorithm to Measure Linear and Rotational Head Acceleration Using Single-Axis Accelerometers. in World Congress of Biomechanics, Munich, Germany.
- Duma, S.M., Manoogian, S.J., Bussone, W.R., Brolinson, P.G., Goforth, M.W., Donnenwerth, J.J., Greenwald, R.M., Chu, J.J., and Crisco, J.J. (2005) Analysis of real-time head accelerations in collegiate football players. *Clin J Sport Med*, 15(1): 3-8.
- Duma, S.M. and Rowson, S. (2009) Every newton hertz: A macro to micro approach to investigating brain injury. *Conf Proc IEEE Eng Med Biol Soc*, 1: 1123-6.
- Eigen, A. M. and Martin, P. G. (2005) Identification of real world injury patterns in aid of dummy development. 19th Enhanced Safety of Vehicles.
- Eisenhauer, J.G. (2003) Regression through the Origin, *Teaching Statistics*, 25(3): 76-80.
- Frieden, T.R., Ikeda, R., Hunt, R.C., Faul, M., Xu, L., Wald, M.M., Coronado, V. (2010) Traumatic Brain Injury in The United States: Emergency Department Visits, Hospitalizations and Deaths 2002 – 2006. National Center for Injury Prevention and Control, Centers for Disease Control and Prevention, U.S. Department of Health and Human Services.
- Gayzik FS, Hamilton CA, Tan JC, et al. (2009) A Multi-Modality Image Data Collection Protocol for Full Body Finite Element Analysis Model Development. SAE Technical Paper 2009-01-2261.
- Gayzik FS, Moreno DP, Danelson KA, McNally C, Klinich KD, Stitzel JD. (2012) External Landmark, Body Surface, and Volume Data of a Mid-Sized Male in Seated and Standing Postures. *Annals of Biomedical Engineering*, 40(9):2019-2032.

- Gennarelli, T.A., Thibault, L.E., and Ommaya, A.K. (1972) Pathophysiologic Responses to Rotational and Translational Accelerations of the Head. *Stapp Car Crash Journal* 16: 296-308.
- Gennarelli, T.A., Thibault, L.E., Adams, J.H., Graham, D.I., Thompson, C.J., and Marcincin, R.P. (1982) Diffuse axonal injury and traumatic coma in the primate. *Annals of Neurology* 12(6): 564-574.
- Gordon, C., et al. (1989) 1988 Anthropometric Survey of U.S. Army Personnel: Methods and Summary Statistics, D.a.E.C. Prepared for United States Army Natick Research, Editor.
- Guskiewicz, K.M., Mihalik, J.P., Shankar, V., Marshall, S.W., Crowell, D.H., Oliaro, S.M., Ciocca, M.F., and Hooker, D.N. (2007) Measurement of head impacts in collegiate football players: relationship between head impact biomechanics and acute clinical outcome after concussion. *Neurosurgery*, 61(6): 1244-53
- Hardy, W.N., Foster, C., Mason, M., Yang, K., King, A., Tashman, S. (2001) Investigation of head injury mechanisms using neutral density technology and high-speed biplanar X-ray. *Stapp Car Crash Journal* 45: 337-368.
- Hardy, W.N., Mason, M.J., Foster, C.D., Shah, C.S., Kopacz, J.M., Yang, K.H., King, A.L., Bishop, J., Bey, M., Anderst, W., Tashman, S. (2007) A Study of the Response of the Human Cadaver Head to Impact. *Stapp Car Crash Journal*, Vol. 51, pp. 17-80.
- Hodgson, V.R., J. Brinn, L.M. Thomas, and S.W. Greenberg. (1970). Fracture behavior of the skull frontal bone against cylindrical surfaces. In 14th *Stapp Car Crash Conference*.
- Holbourn, A.H.S. (1943) Mechanics of head injury. *Lancet* 2, October 9: 438-441.
- Hertz, E. (1993) A note on the head injury criterion (HIC) as a predictor of the risk of skull fracture. *Proceedings of the 37th Association for the Advancement of Automotive Medicine*: 303-10.
- Manoogian, S., McNeely, D., Duma, S., Brolinson, G., and Greenwald, R. (2006) Head acceleration is less than 10 percent of helmet acceleration in football impacts. *Biomed Sci Instrum*, vol. 42: 383-388.
- Mao H, Zhang L, Jiang B, et al. (2013) Development of a Finite Element Human Head Model Validated With Forty Nine Loading Cases From Experimental and Real World Impacts. *J Biomech Eng*.:10.1115/1.4025101.
- Meaney, D.F, Smith, D., Ross, D.T., and Gennarelli, T.A. (1993) Diffuse axonal injury in the miniature pig: Biomechanical development and injury threshold. *ASME Crashworthiness and occupant protection in transportation systems* 25: 169-175.
- Nahum, A.M., R. Smith, and C.C. Ward. (1977). Intracranial pressure dynamics during head impact. In *Proc. 21st Stapp Car Crash Conference*, SAE Paper No. 770922.
- NHTSA (1995) Final economic assessment, FMVSS No. 201, upper interior head protection. www.regulations.gov, NHTSA docket 1996-1762-0003.
- Nusholtz, G.S., Lux, P., Kaiker, P., and Janicki, M.A., (1984) Head impact response skull deformation and angular accelerations. *Proc. 28th Stapp Car Crash Conference*, pp. 41-74, Society of Automotive Engineers, Warrendale, PA.
- Nyquist, G.W., J.M. Cavanaugh, S.J. Goldberg, and A.I. King. (1986). Facial impact tolerance and response. In *Proc. 30th Stapp Car Crash Conference*, SAE Paper No. 861896.
- Ommaya A.K. (1985) Biomechanics of Head Injury: Experimental Aspects, in "The Biomechanics of Trauma" edited by Nahum A.M. and Melvin J.W., pp 245 – 269.
- Rowson, S., Brolinson, G., Goforth, M., Dietter, D., and Duma, S.M. (2009) Linear and angular head acceleration measurements in collegiate football. *J Biomech Eng*, 131(6): 061016.
- Rowson, S., Duma, S. M., Beckwith, J. G., Chu, J. J., Greenwald, R. M., Crisco, J. J., Brolinson, P. G., Duhaime, A-C., McAlister, T. W., Maerlender, A. C., (2011) Rotational Head Kinematics in Football Impacts: An Injury Risk Function for Concussion, *Annals of Biomedical Eng*.: 1-13.
- SAS, Version 9.3, Cary, NC.
- Stalnaker, R.L., Alem, N.M., Benson, J.B., Melvin, J.W. (1977) Validation studies for head impact injury model. Final report DOT HS-802 566, National Highway Traffic Safety Administration, US, Department of Transportation, Washington, DC.
- Takhounts, E.G., Eppinger, R.H., Campbell, J.Q., Tannous, R.E., Power, E.D., Shook, L.S. (2003a)

On the Development of the SIMon Finite Element Head Model. Stapp Car Crash Journal 47: 107-133.

Takhounts, E.G., Crandall, J.R., Darvish, K.K. (2003b) On the importance of nonlinearity of brain tissue under large deformations. Stapp Car Crash Journal 47:79-92.

Takhounts, E.G., Hasija, V., Ridella, S.A., Tannous, R.E., Campbell, J.Q., Malone, D., Danelson, K., Stitzel, J., Rowson, S., Duma, S, (2008) Investigation of Traumatic Brain Injuries Using the Next Generation of Simulated Injury Monitor (SIMon) Finite Element Head Model. Stapp Car Crash Journal 52: 1-32.

Takhounts, E.G., Hasija, V., Ridella, S.A., Rowson, S, Duma, S.M. (2011) Kinematic Rotational Brain Injury Criterion (BRIC). Proc. 22nd ESV Conference.

Trosseille, X., et al. (1992) Development of a F.E.M. of the Human Head According to a Specific Test Protocol, 36th Stapp Car Crash Conference Proceedings, SAE Paper No.922527.

Ueno, K., and Melvin, J.W. (1995) Finite element model study of head impact based on hybrid III head acceleration: The effects of rotational and translational accelerations. J. Biomech Eng. 117(3): 319-328.

APPENDIX 0

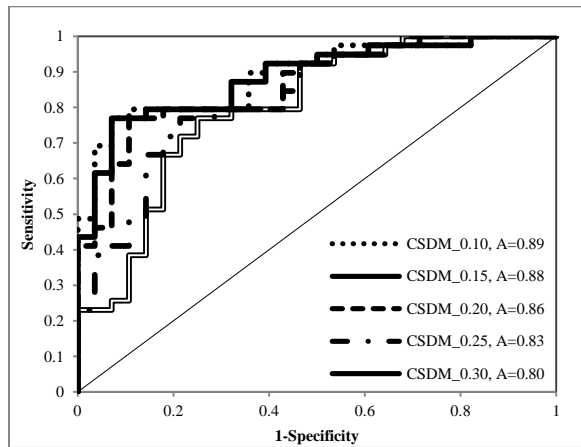


Figure 0.1. ROC curves for various thresholds of CSDM with associated areas under the ROC curve.

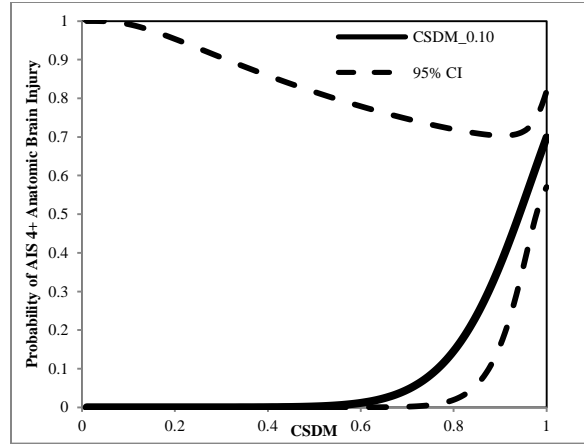


Figure 0.2. Risk of AIS 4+ anatomic brain injuries in animal tests as a function of CSDM (strain threshold = 0.10).

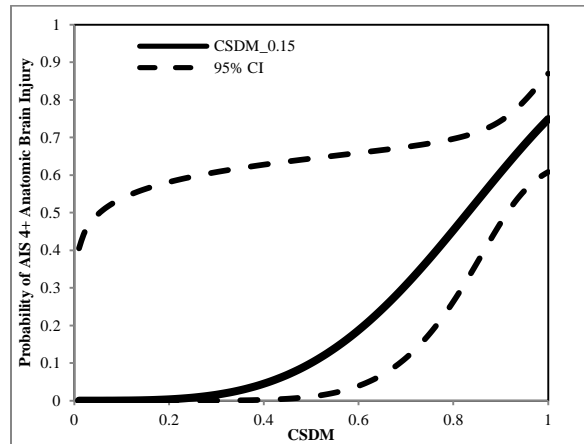


Figure 0.3. Risk of AIS 4+ anatomic brain injuries in animal tests as a function of CSDM (strain threshold = 0.15).

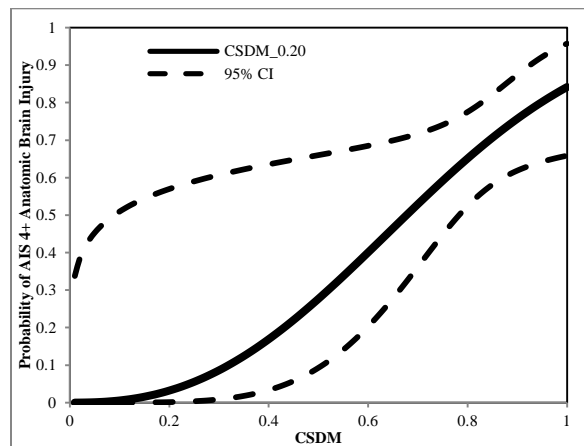


Figure 0.4. Risk of AIS 4+ anatomic brain injuries in animal tests as a function of CSDM (strain threshold = 0.20).

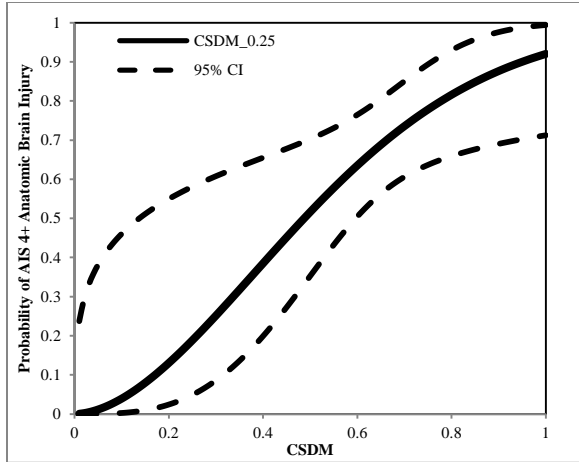


Figure 0.5. Risk of AIS 4+ anatomic brain injuries in animal tests as a function of CSDM (strain threshold = 0.25).

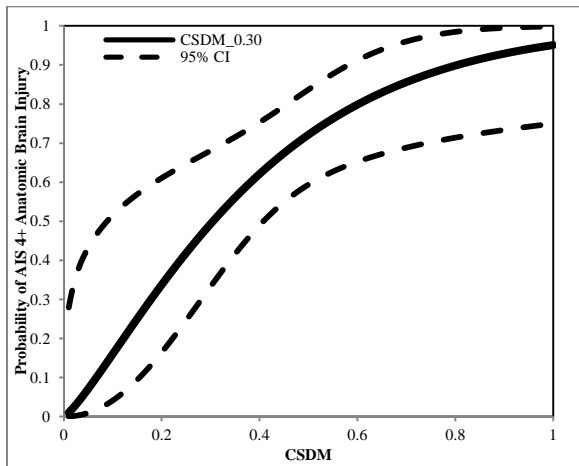


Figure 0.6. Risk of AIS 4+ anatomic brain injuries in animal tests as a function of CSDM (strain threshold = 0.30).

APPENDIX I

Below are correlation figures between physical (max pressure, CSDM, and max principal strain) and kinematic parameters (HIC15, max resultant linear acceleration, max resultant angular acceleration, and max resultant angular velocity) for pendulum tests for all ATDs - Hybrid III 50th Male, Hybrid III 5th Female, THOR 50th Male, ES-2re, SID-IIs, WorldSID 50th Male, and WorldSID 5th Female.

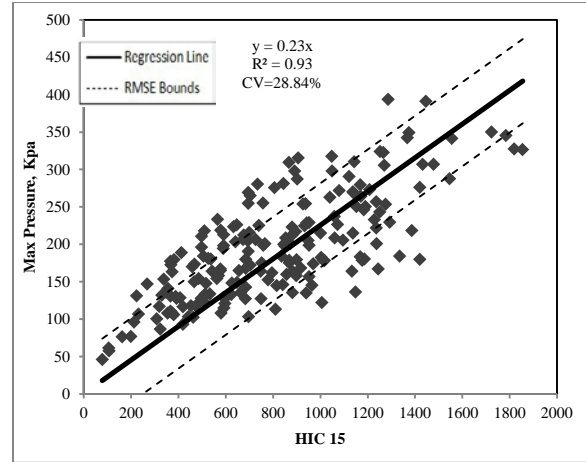


Figure I.1. Max Pressure versus HIC15.

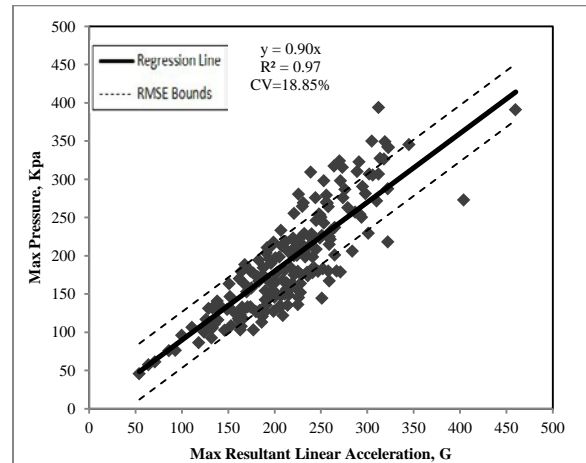


Figure I.2. Max Pressure versus Max Resultant Linear Acceleration.

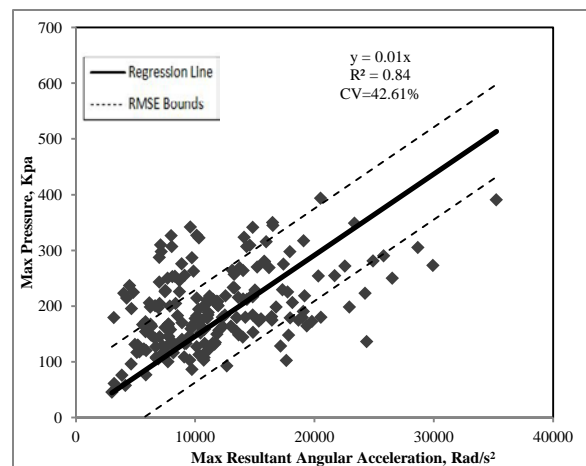


Figure I.3. Max Pressure versus Max Resultant Angular Acceleration.

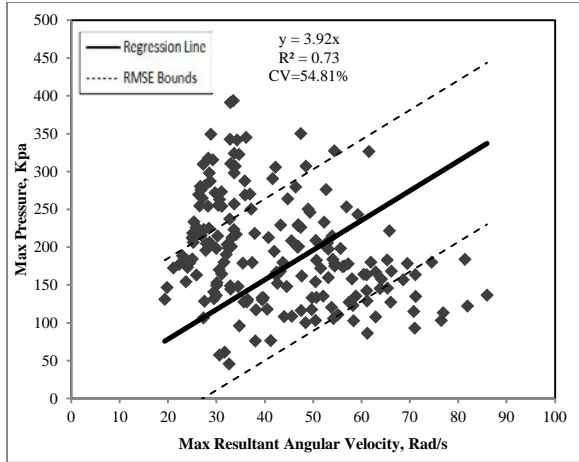


Figure I.4. Max Pressure versus Max Resultant Angular Velocity.

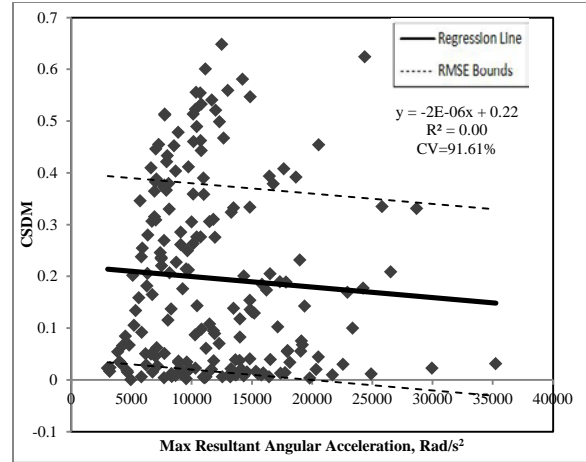


Figure I.7. CSDM versus Max Resultant Angular Acceleration.

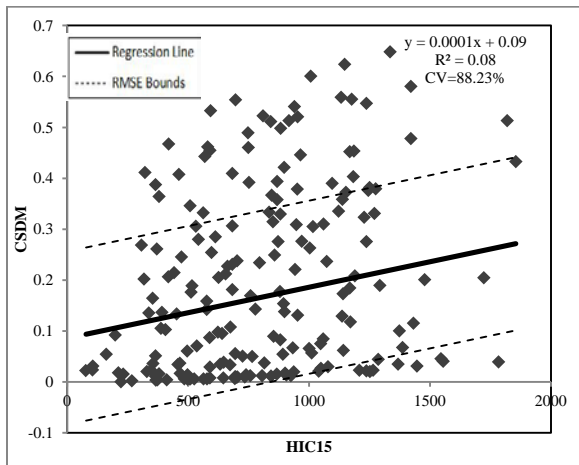


Figure I.5. CSDM versus HIC15.

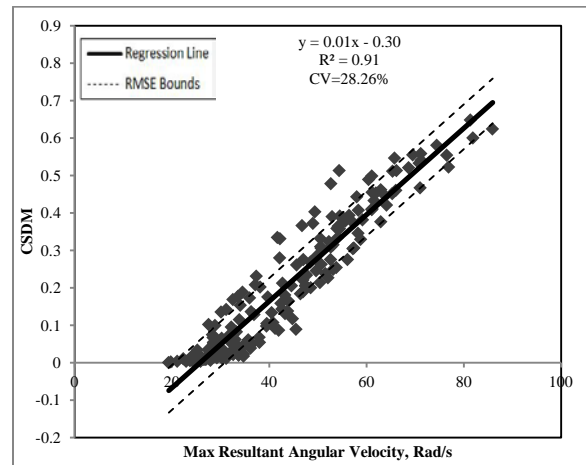


Figure I.8. CSDM versus Max Resultant Angular Velocity.

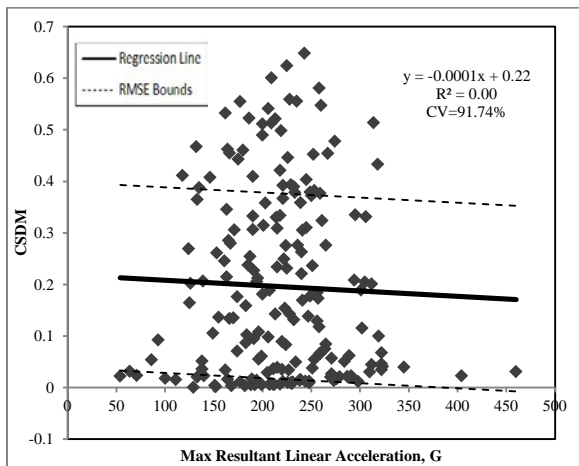


Figure I.6. CSDM versus Max Resultant Linear Acceleration.

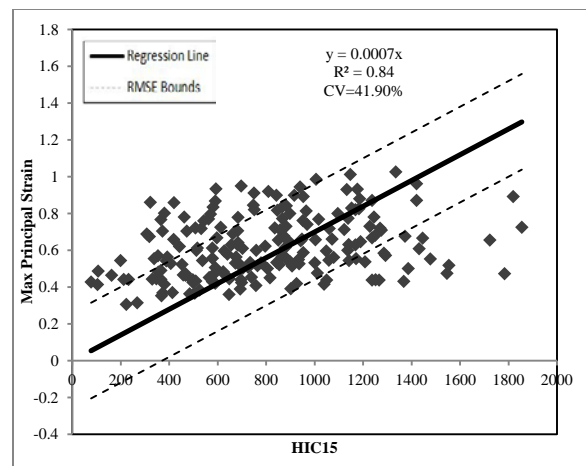


Figure I.9. MPS versus HIC15.

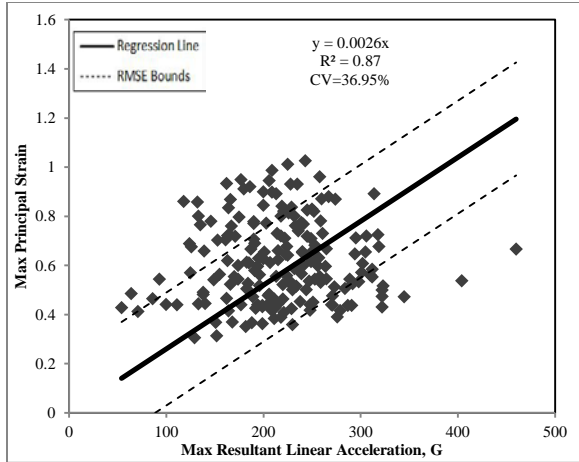


Figure I.10. MPS versus Max Resultant Linear Acceleration.

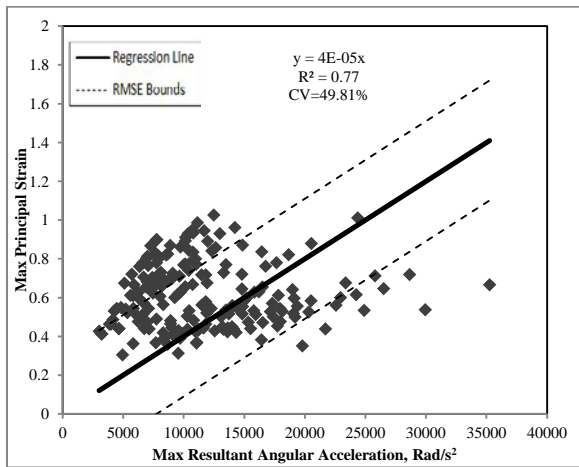


Figure I.11. MPS versus Max Resultant Angular Acceleration.

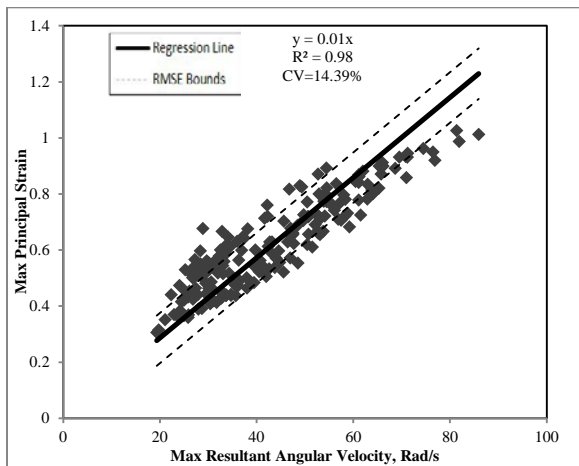


Figure I.12. MPS versus Max Resultant Angular Velocity.

APPENDIX II

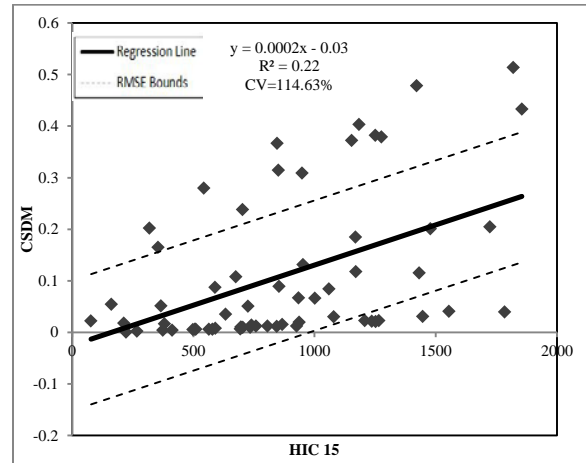


Figure II.1. CSDM vs. HIC 15 for HIII 50th percentile male ATD (all impact conditions).

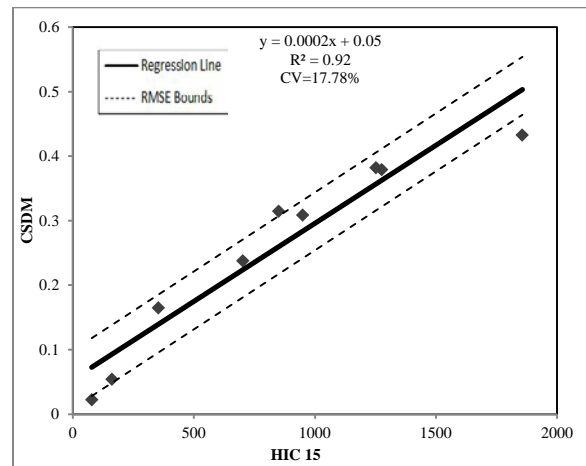


Figure II.2. CG, 0 degrees, padded.

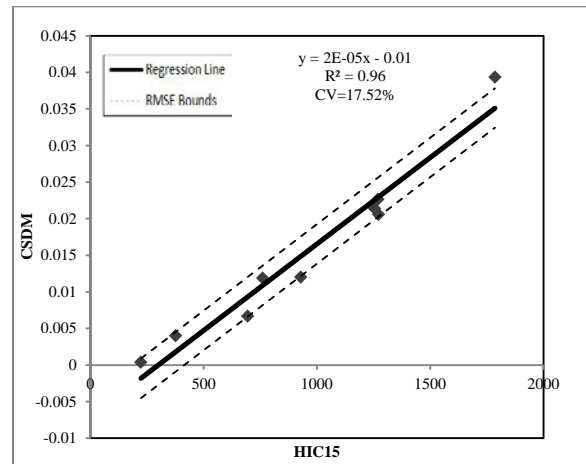


Figure II.3. CG, 0 degrees, unpadded.

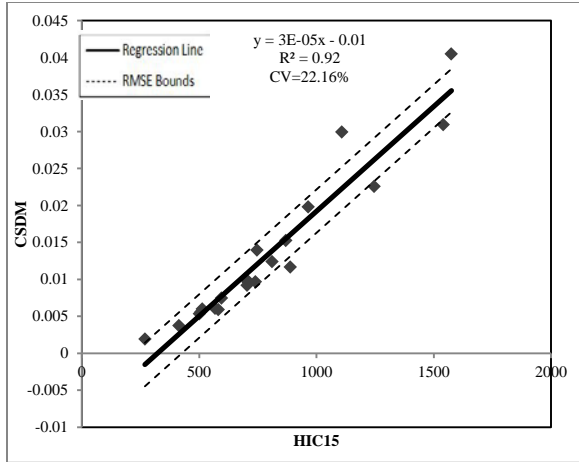


Figure II.4. Forehead, 0 degrees, unpadded.

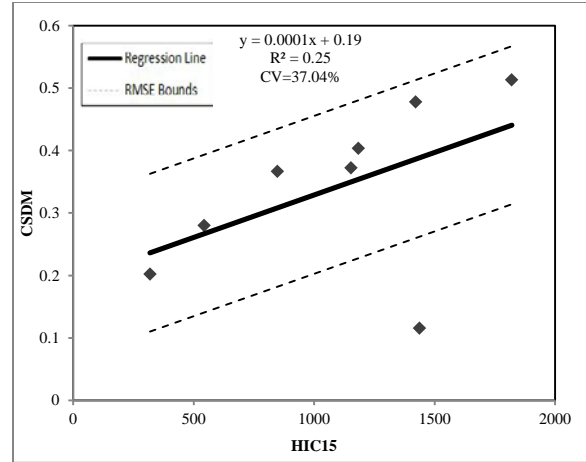


Figure II.7. CG, 30 degrees, padded.

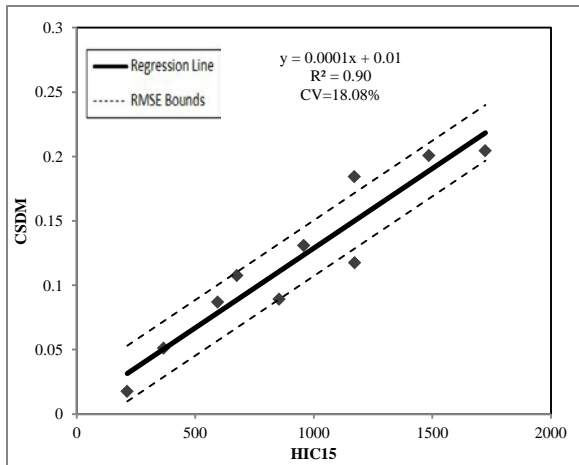


Figure II.5. Forehead, 0 degrees, padded.

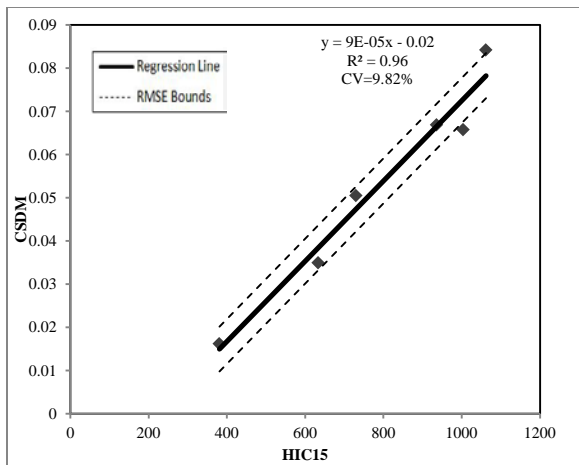


Figure II.6. CG, 30 degrees, unpadded.

APPENDIX III

Table III.1. Risk curve equations for Figure 15.

$P(AIS\ 1) = 1 - e^{-\left(\frac{CSDM}{0.060}\right)^{1.8}}$
$P(AIS\ 2) = 1 - e^{-\left(\frac{CSDM}{0.300}\right)^{1.8}}$
$P(AIS\ 3) = 1 - e^{-\left(\frac{CSDM}{0.490}\right)^{1.8}}$
$P(AIS\ 4) = 1 - e^{-\left(\frac{CSDM}{0.600}\right)^{1.8}}$
$P(AIS\ 5) = 1 - e^{-\left(\frac{CSDM}{0.624}\right)^{1.8}}$

Table III.2. Risk curve equations for Figure 16.

$P(AIS\ 1) = 1 - e^{-\left(\frac{MPS}{0.101}\right)^{2.84}}$
$P(AIS\ 2) = 1 - e^{-\left(\frac{MPS}{0.505}\right)^{2.84}}$
$P(AIS\ 3) = 1 - e^{-\left(\frac{MPS}{0.828}\right)^{2.84}}$
$P(AIS\ 4) = 1 - e^{-\left(\frac{MPS}{1.010}\right)^{2.84}}$
$P(AIS\ 5) = 1 - e^{-\left(\frac{MPS}{1.050}\right)^{2.84}}$

Table III.3. Risk curve equations for Figure 17.

$P(AIS\ 1) = 1 - e^{-\left(\frac{BrIC-0.51}{0.060}\right)^{1.8}}$
$P(AIS\ 2) = 1 - e^{-\left(\frac{BrIC-0.51}{0.301}\right)^{1.8}}$
$P(AIS\ 3) = 1 - e^{-\left(\frac{BrIC-0.51}{0.493}\right)^{1.8}}$
$P(AIS\ 4) = 1 - e^{-\left(\frac{BrIC-0.51}{0.601}\right)^{1.8}}$
$P(AIS\ 5) = 1 - e^{-\left(\frac{BrIC-0.51}{0.625}\right)^{1.8}}$

Table III.4. Risk curve equations for Figure 18.

$P(AIS\ 1) = 1 - e^{-\left(\frac{BrIC-0.523}{0.065}\right)^{1.8}}$
$P(AIS\ 2) = 1 - e^{-\left(\frac{BrIC-0.523}{0.324}\right)^{1.8}}$
$P(AIS\ 3) = 1 - e^{-\left(\frac{BrIC-0.523}{0.531}\right)^{1.8}}$
$P(AIS\ 4) = 1 - e^{-\left(\frac{BrIC-0.523}{0.647}\right)^{1.8}}$
$P(AIS\ 5) = 1 - e^{-\left(\frac{BrIC-0.523}{0.673}\right)^{1.8}}$

Table III.5. Risk curve equations for Figure 19.

$P(AIS\ 1) = 1 - e^{-\left(\frac{BrIC}{0.113}\right)^{2.84}}$
$P(AIS\ 2) = 1 - e^{-\left(\frac{BrIC}{0.567}\right)^{2.84}}$
$P(AIS\ 3) = 1 - e^{-\left(\frac{BrIC}{0.929}\right)^{2.84}}$
$P(AIS\ 4) = 1 - e^{-\left(\frac{BrIC}{1.134}\right)^{2.84}}$
$P(AIS\ 5) = 1 - e^{-\left(\frac{BrIC}{1.179}\right)^{2.84}}$

Table III.6. Risk curve equations for Figure 20.

$P(AIS\ 1) = 1 - e^{-\left(\frac{BrIC}{0.120}\right)^{2.84}}$
$P(AIS\ 2) = 1 - e^{-\left(\frac{BrIC}{0.602}\right)^{2.84}}$
$P(AIS\ 3) = 1 - e^{-\left(\frac{BrIC}{0.987}\right)^{2.84}}$
$P(AIS\ 4) = 1 - e^{-\left(\frac{BrIC}{1.204}\right)^{2.84}}$
$P(AIS\ 5) = 1 - e^{-\left(\frac{BrIC}{1.252}\right)^{2.84}}$